サブミリ波突発天体・時間軸天文学

冨永望

（国立天文台）

松岡さん（ASIAA）、岩田さん（水沢VLBI）、前田さん（京大）に意見を伺いました。

2024/12/27

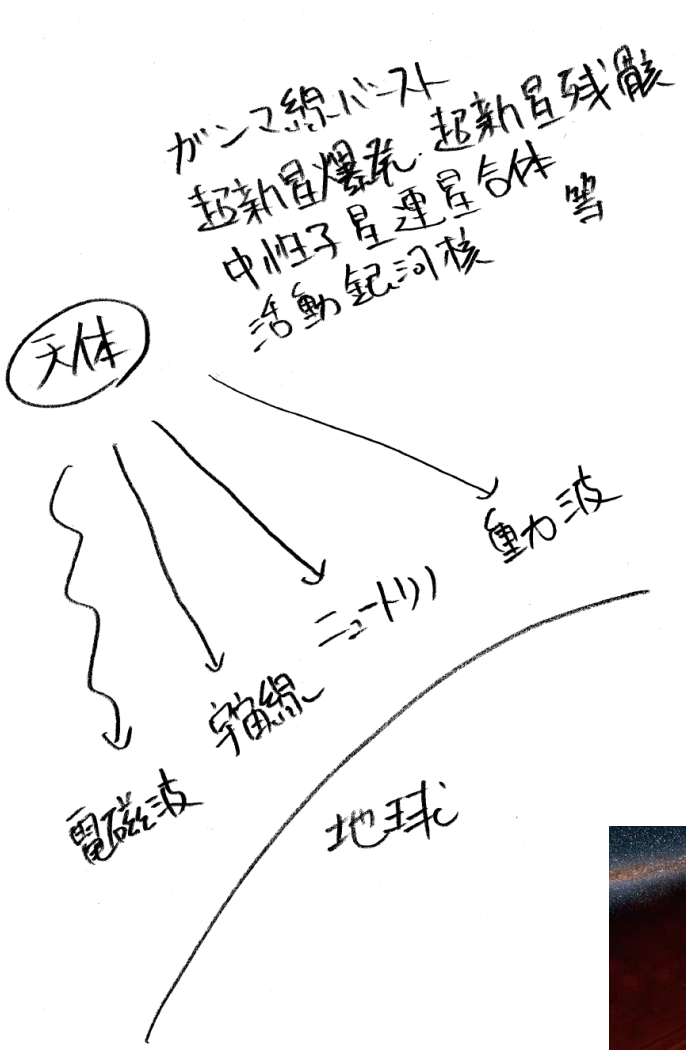
ASTE Science and Development Workshop 2024

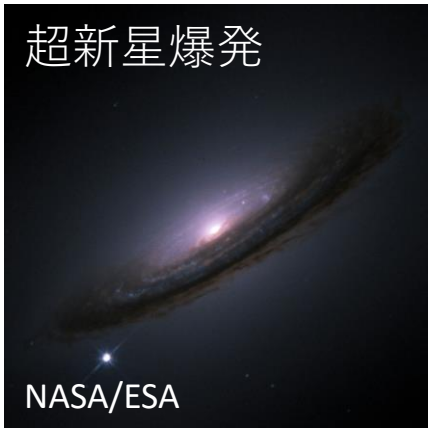
時間軸天文学

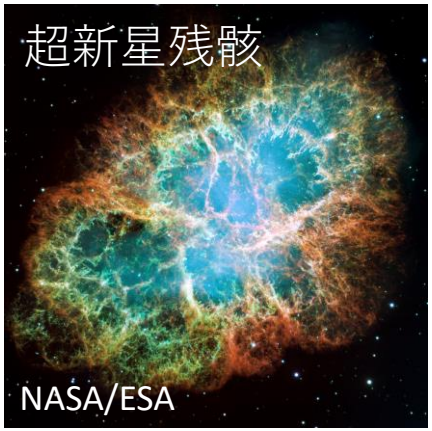
研究対象

- Variables
  - Variable stars
    - Cepheids
    - Mira variables
  - Flares of dwarf stars
  - Cataclysmic variables
  - Recurrent novae
- Transients
  - Supernovae
  - Kilonovae/Macronovae
  - Gamma-ray bursts
  - Fast radio bursts?

マルチメッセンジャー天文学

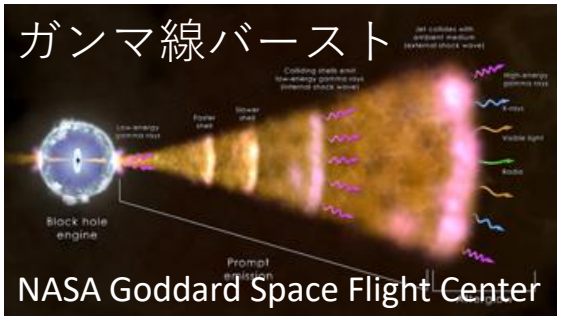












Transients

- いつどこで起こるのかわからない
- ある天体のある時刻の観測は一度しか行えない

→ どんな小口径望遠鏡でも唯一無二の貢献が可能。だが事前準備が必要不可欠

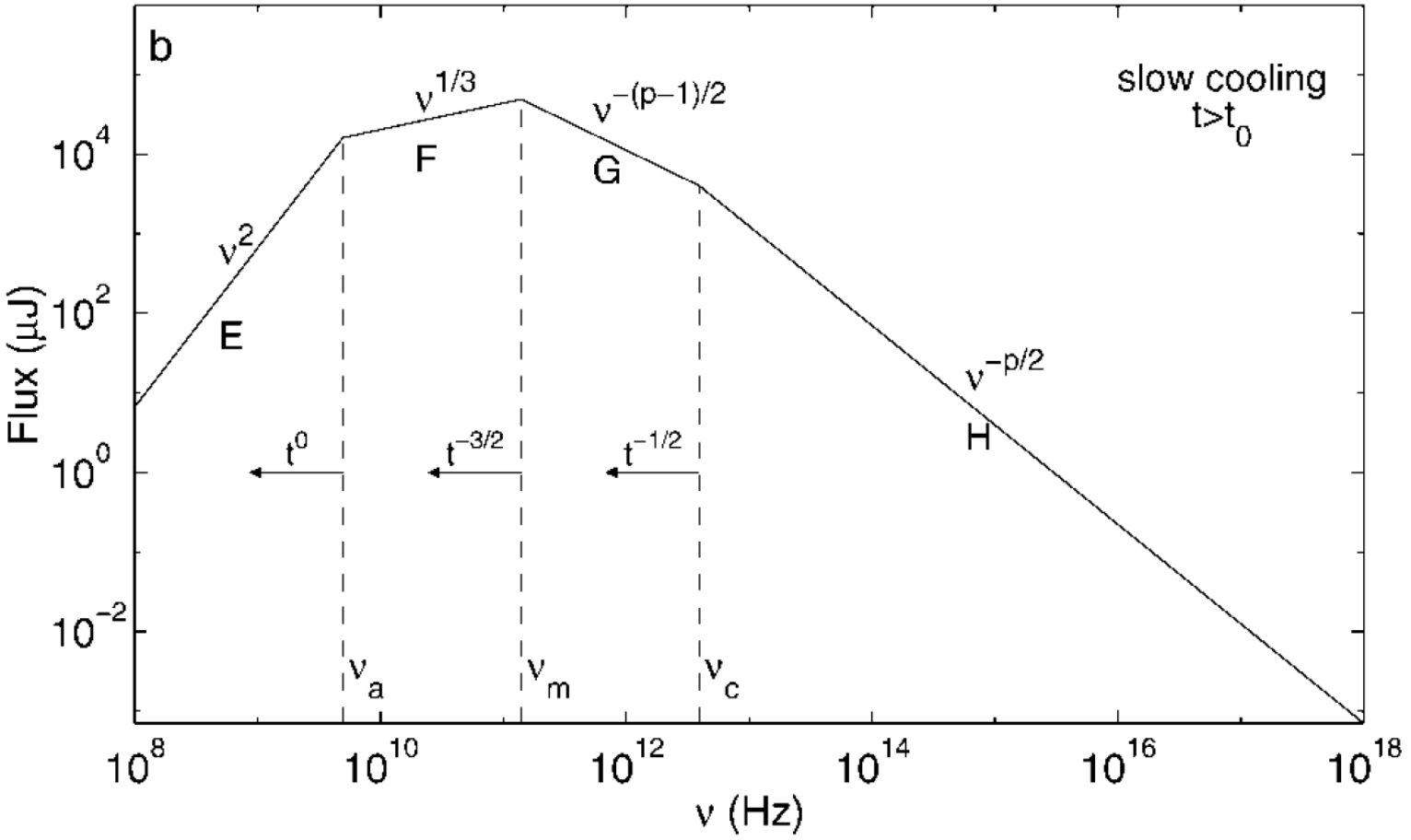


http://www.dailymail.co.uk/sciencetech/article-2074145/Supernova-SN-2011fe-spotted-just-11-hours-exploded.html

Transients

Radio emission from transients

- Synchrotron emission



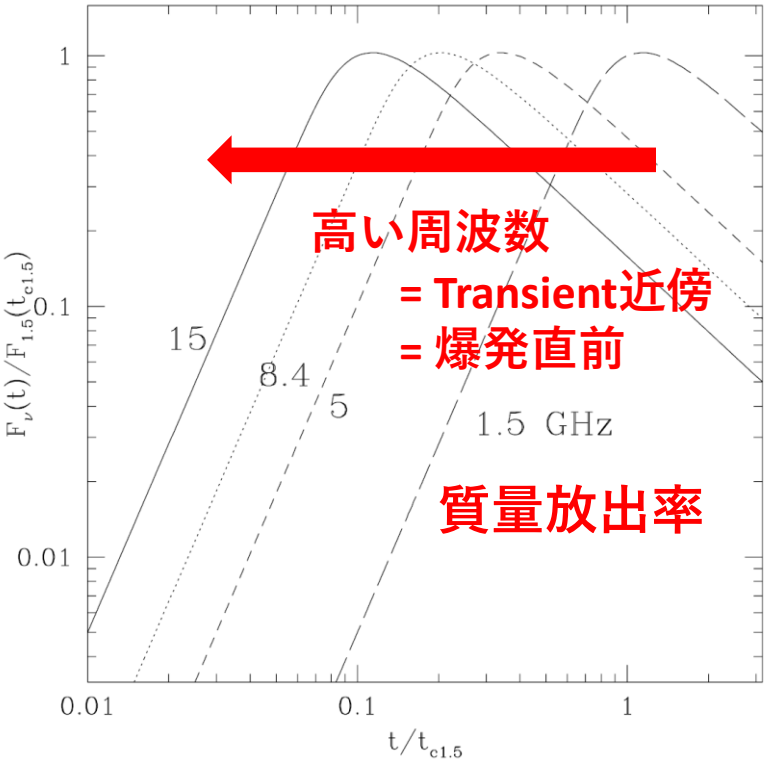
Sari+98

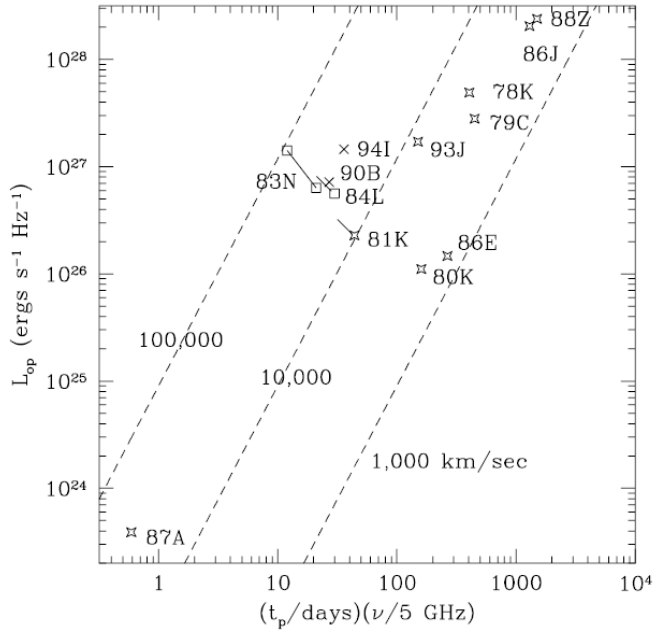
Key parameters

- Synchrotron self-absorption (free-free absorption)
- Cooling timescale

$$\frac{F_\nu(t)}{F_{\nu_c}(t_c)} = 1.582\left(\frac{t}{t_c}\right)^a\left(\frac{\nu}{\nu_c}\right)^{5/2} \times\left\{1-\exp\left[-\left(\frac{t}{t_c}\right)^{-(a+b)}\left(\frac{\nu}{\nu_c}\right)^{-(\gamma+4)/2}\right]\right\}.$$

a,b: structure of ejecta and CSM





Chevalier82;98

Core-collapse supernovae

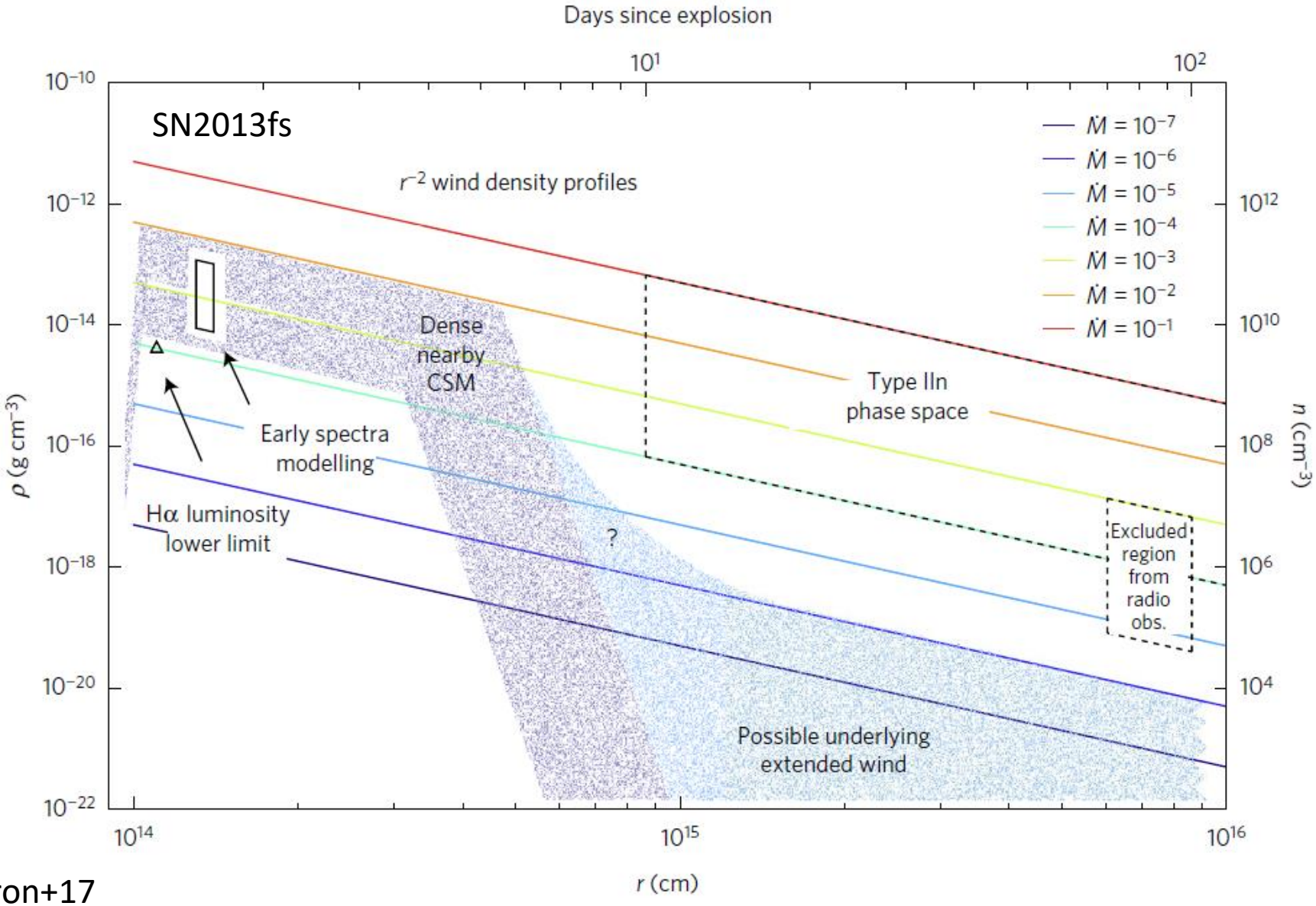
Last moment of massive star



NASA's Goddard Space Flight Center
Video courtesy of ESA/Hubble/L. Calcada

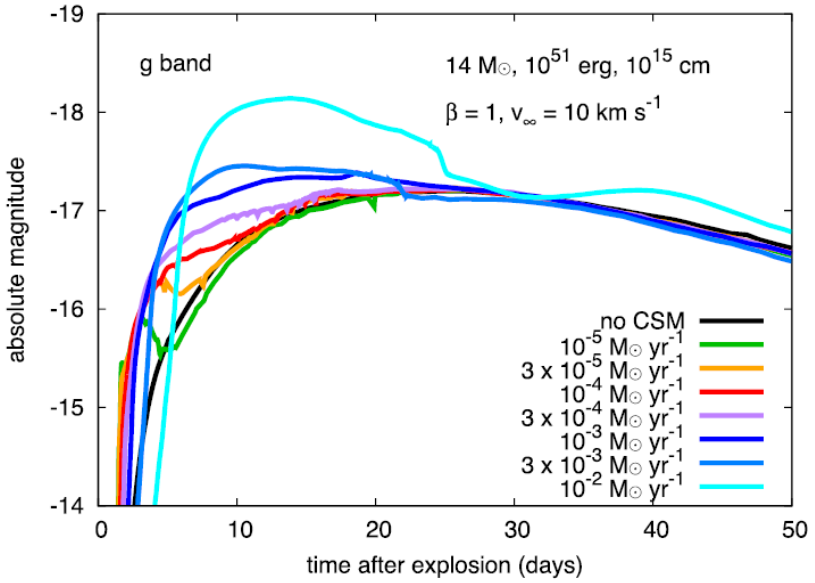
https://svs.gsfc.nasa.gov/11447

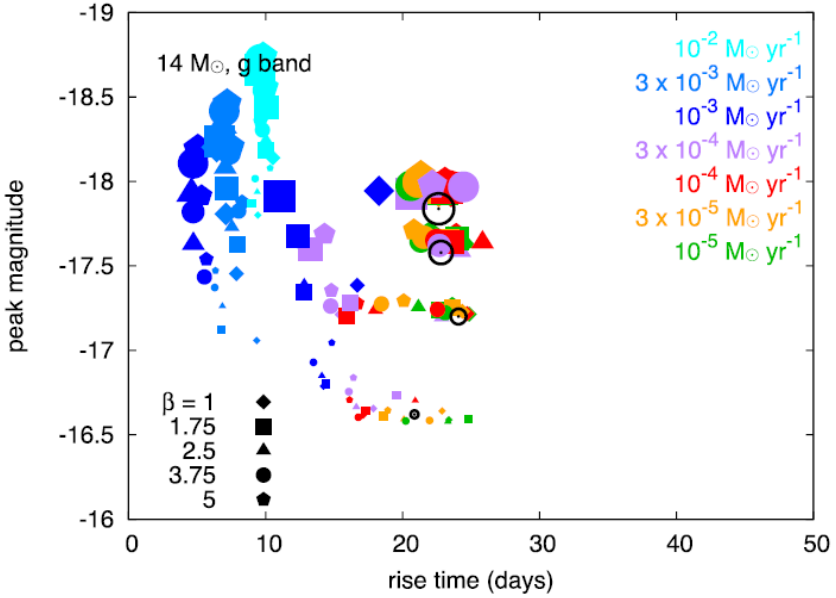
Supernovae in dense CSM

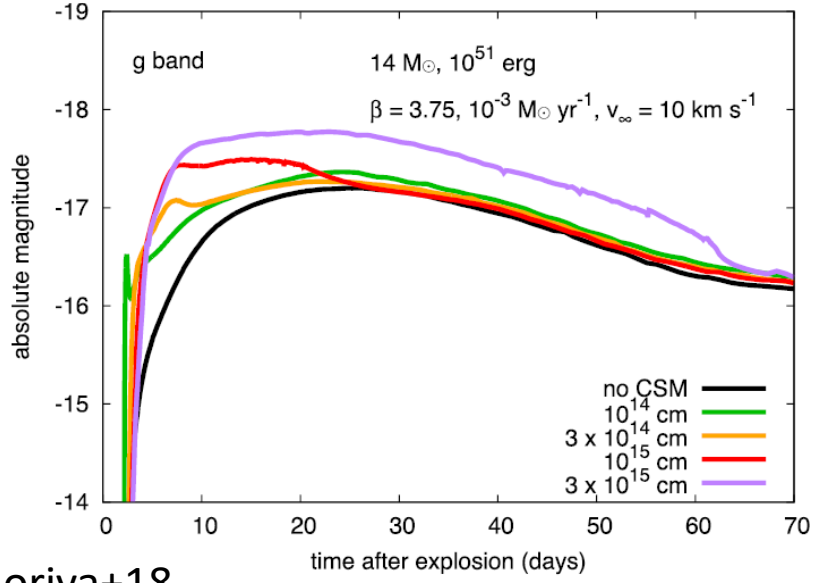


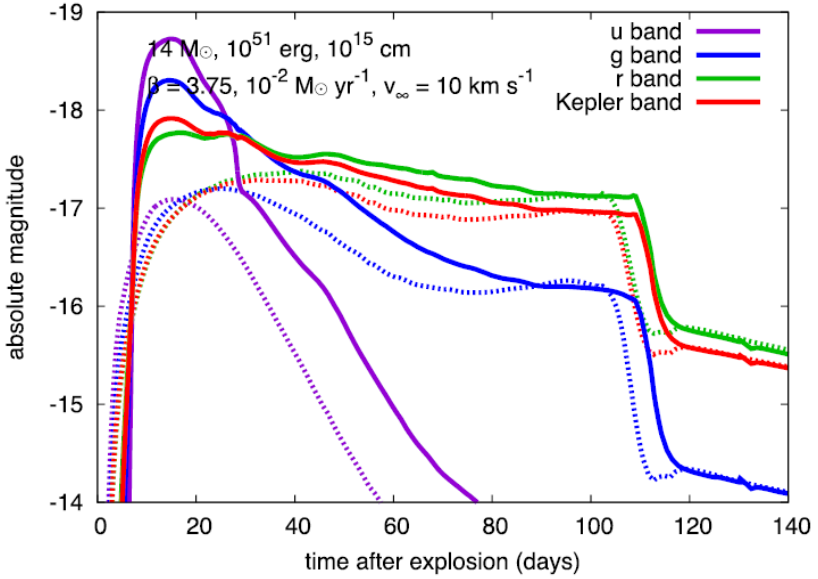
Yaron+17

SNe IIP with dense CSM



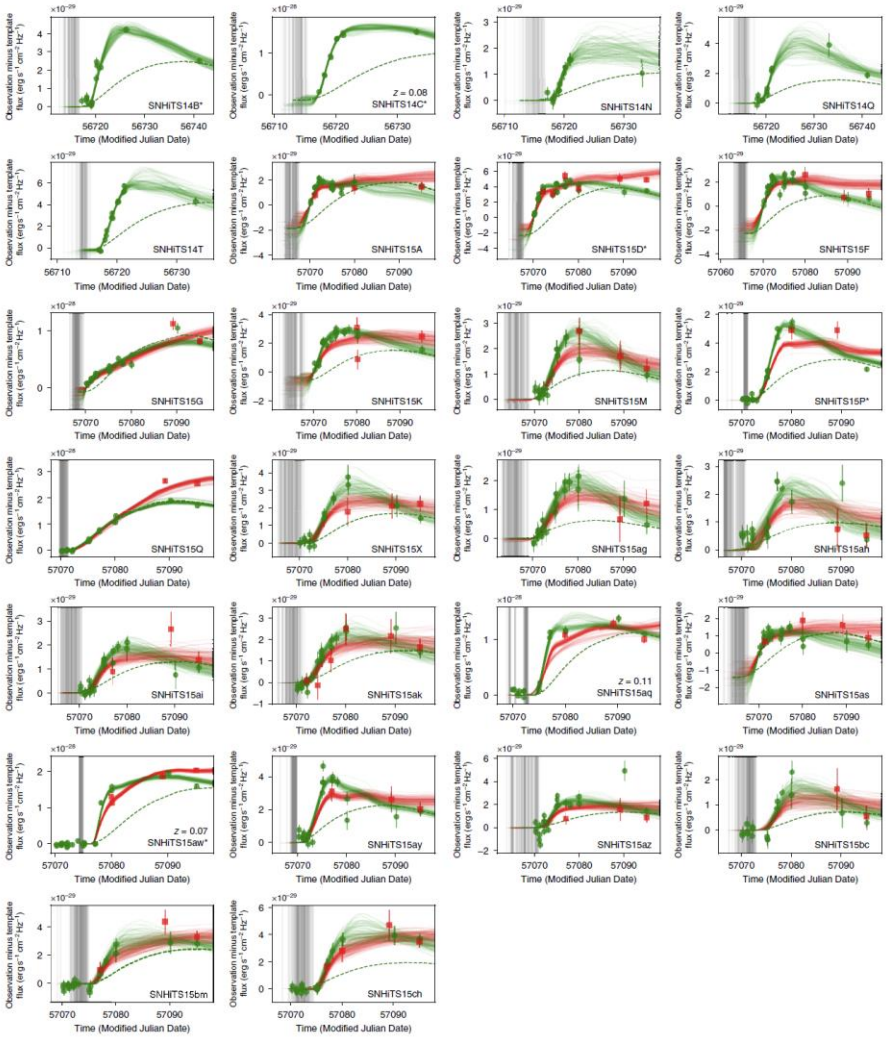






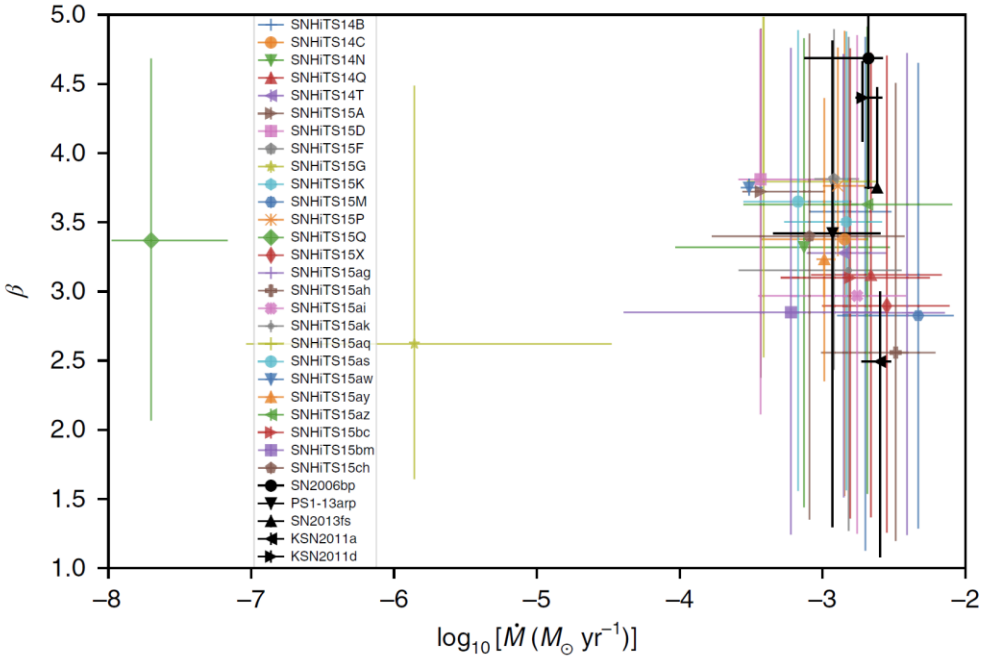
Moriya+18

High Cadence Transient Survey (HiTS) with CTIO/DECam



Assuming SNe with dense CSM

Forster+18

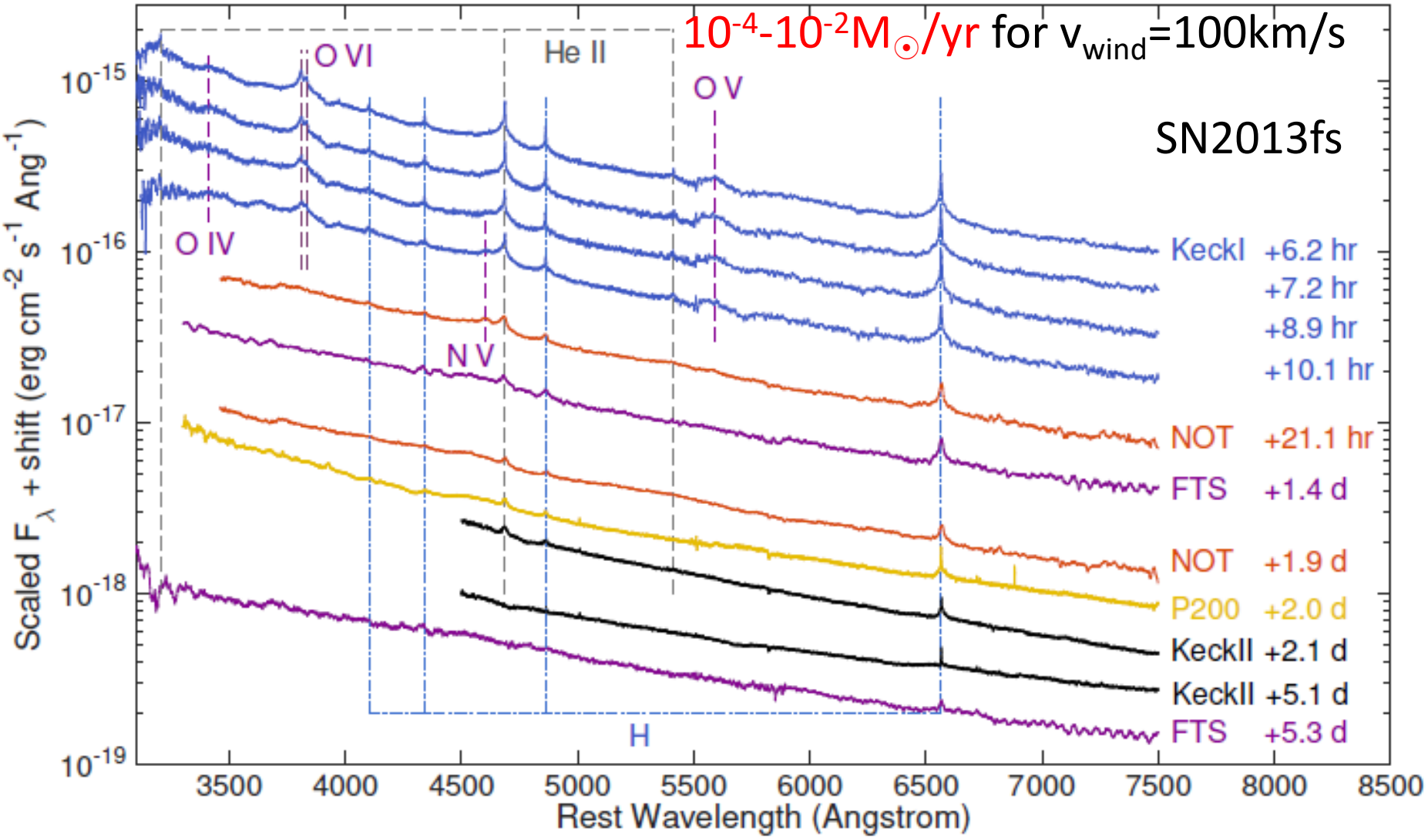


- 26 rising transients (24 transients are rapid |dm/dt| > 0.2mag/day)
- Detection efficiency: 28 % for low M_{dot}, 72% for high M_{dot}
- **1/5** of CCSNe could be without dense CSM.

SN2013fs -evidence of dense CSM-

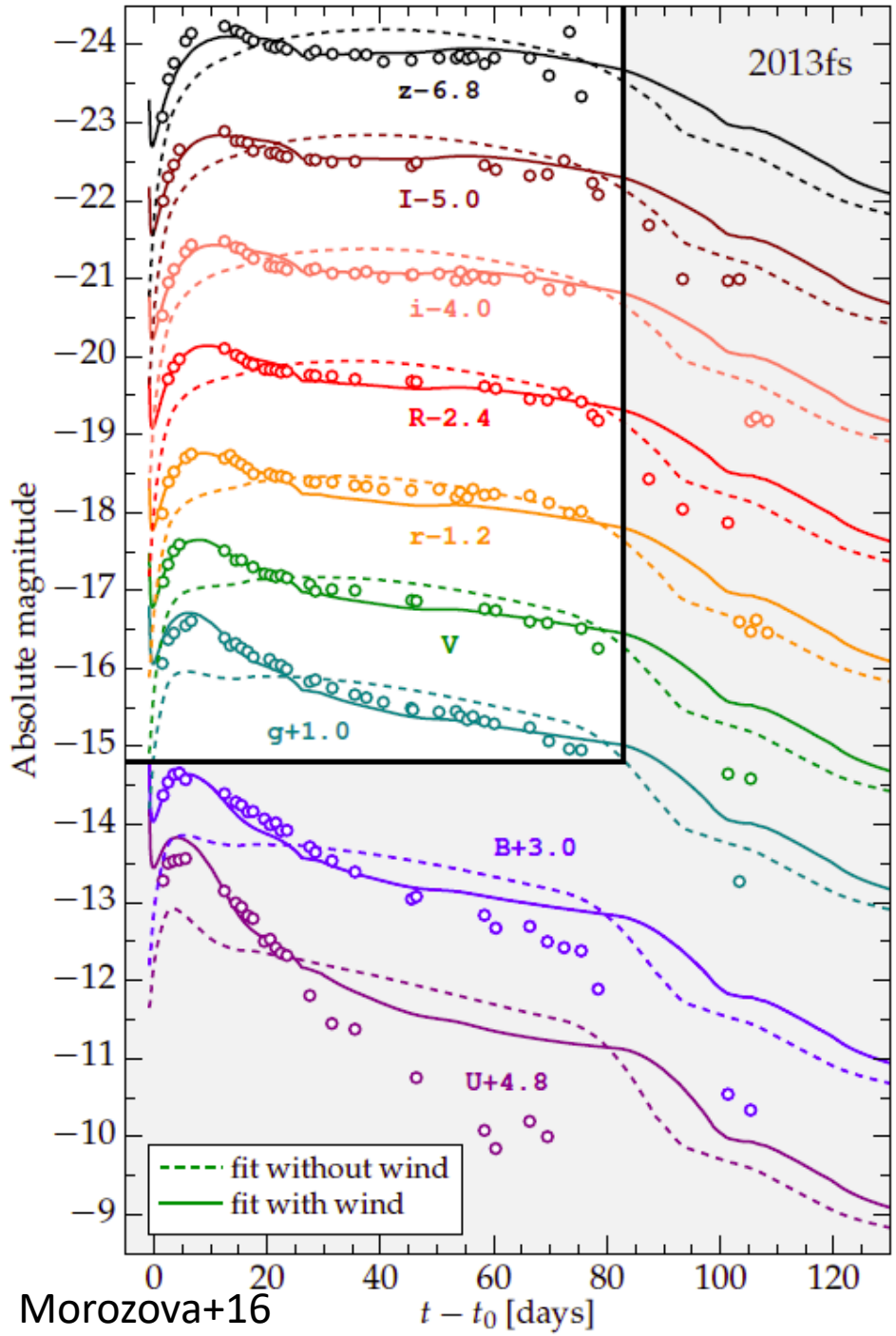
Mass loss rate:

10^{-4}-$10^{-2}M_{\odot}$/yr for v_{wind}=100km/s

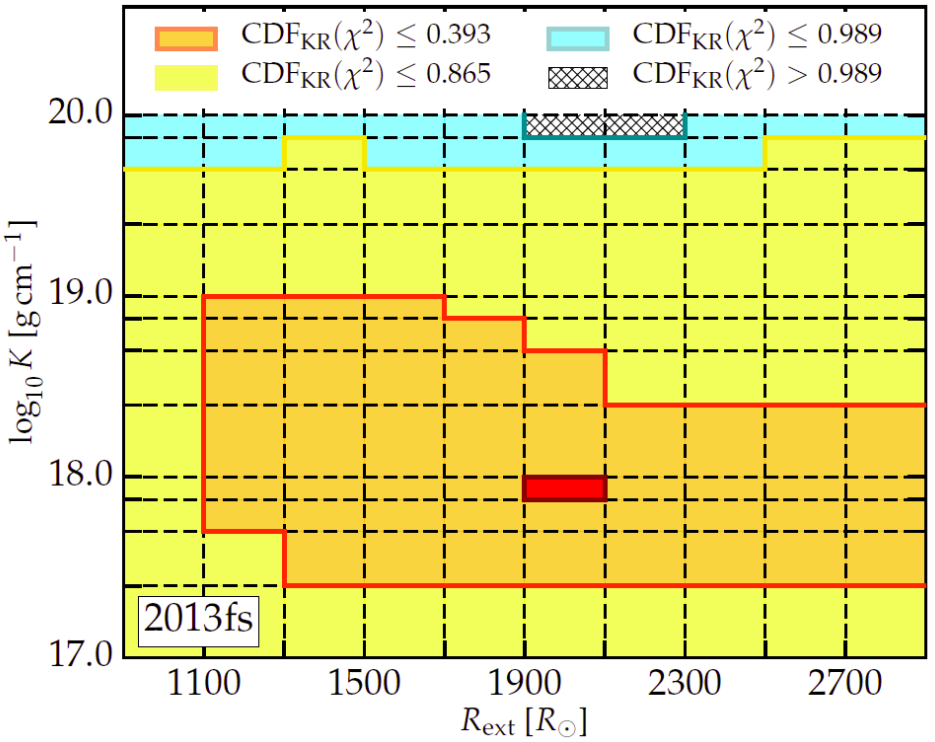


Yaron+17

SNe with dense CSM SN2013fs



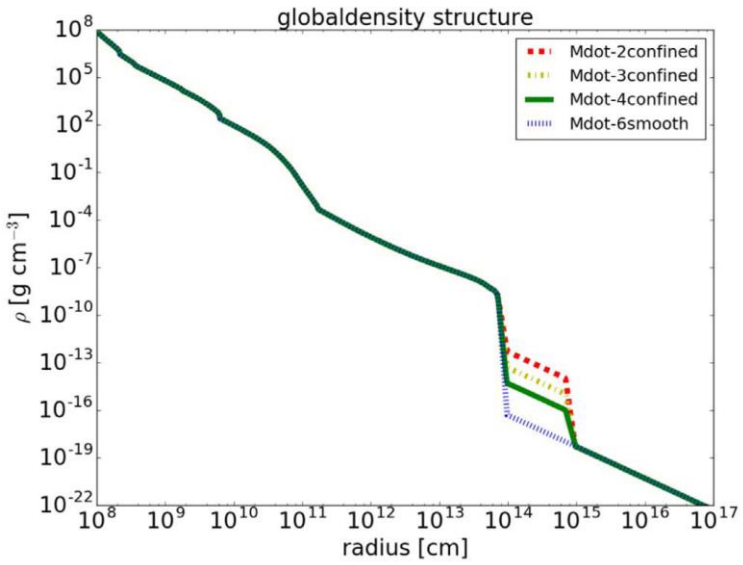
Morozova+16

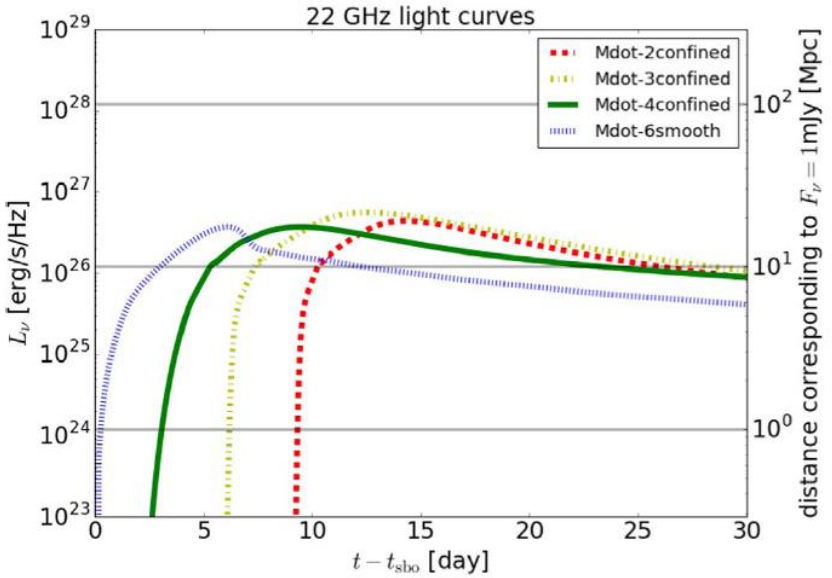


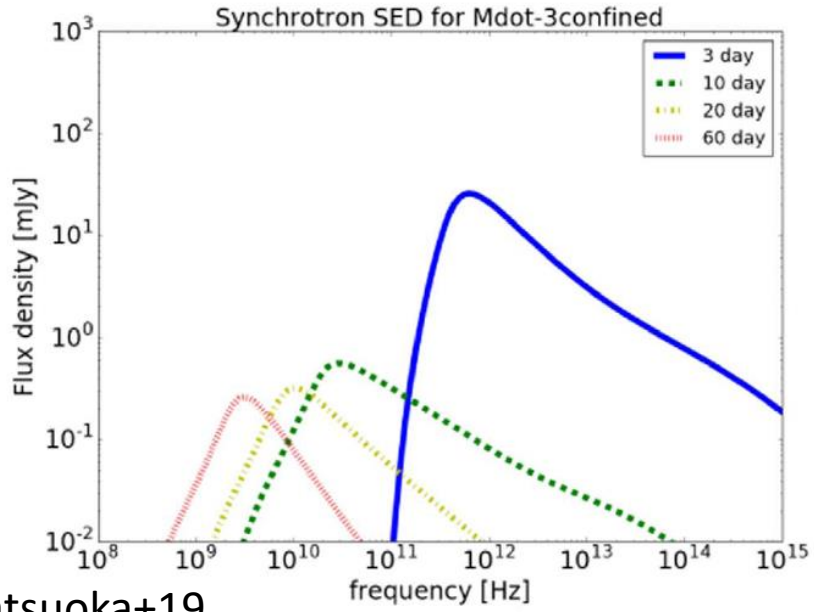
Mass loss rate:

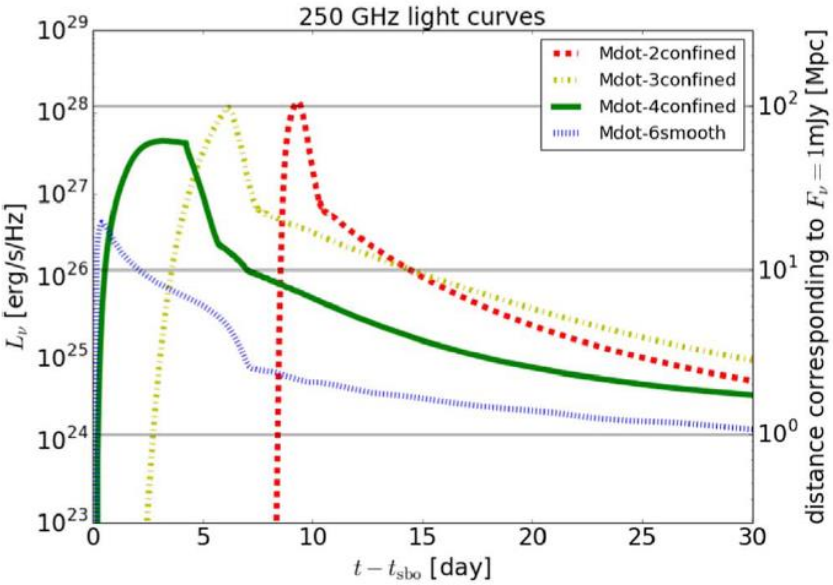
$1.5 M_\odot$/yr for v_{wind}=100km/s

Radio Emission from Supernovae in the Very Early Phase: Implications for the Dynamical Mass Loss of Massive Stars









Matsuoka+19

The Astrophysical Journal Letters, 951:L31 (5pp), 2023 July 10 https://doi.org/10.3847/2041-8213/ace0c4
© 2023. The Author(s). Published by the American Astronomical Society.
OPEN ACCESS

Millimeter Observations of the Type II SN 2023ixf: Constraints on the Proximate Circumstellar Medium

@6.9Mpc

Edo Berger[1], Garrett K. Keating[1], Raffaella Margutti[2,3], Keiichi Maeda[4], Kate D. Alexander[5], Yvette Cendes[1], Tarraneh Eftekhari[6,10], Mark Gurwell[1], Daichi Hiramatsu[1], Anna Y. Q. Ho[7], Tanmoy Laskar[8,9], Ramprasad Rao[1], and Peter K. G. Williams[1]

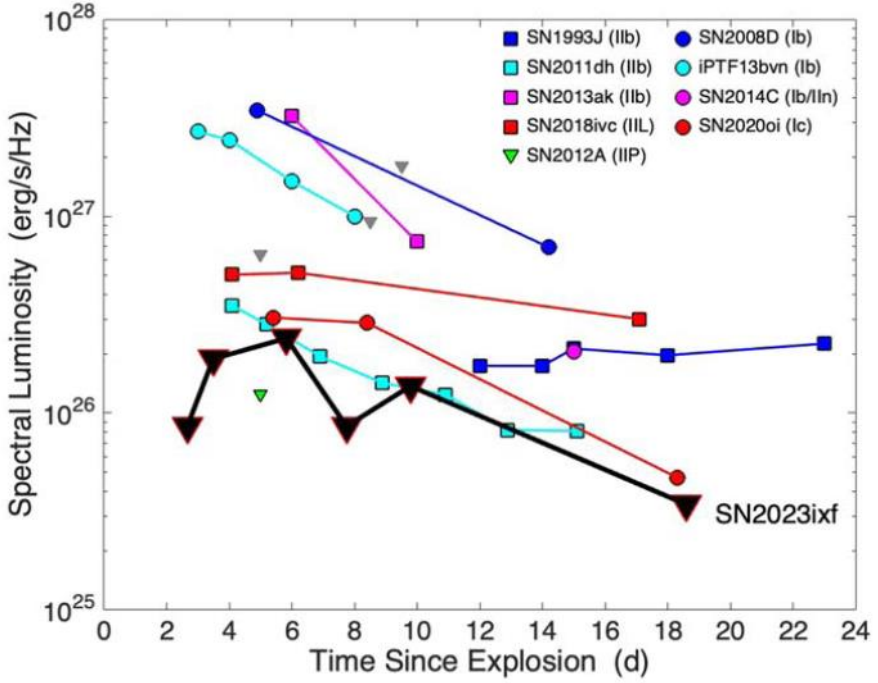


Figure 2. SMA 230 GHz upper limits for SN 2023ixf (black triangles; 3σ) compared to the existing sample of CCSNe with early millimeter-band detections (squares: Type II; circles: Type Ib/c; Weiler et al. 2007; Soderberg et al. 2008; Gorosabel et al. 2010; Chakraborti et al. 2013; Horesh et al. 2013a, 2013b; Zauderer et al. 2013b, 2014; Maeda et al. 2021), or upper limits (triangles; Carpenter 2010; Horesh et al. 2012b, 2012a; Zauderer et al. 2013a); we particularly highlight the nondetection of the Type IIP SN 2012A.

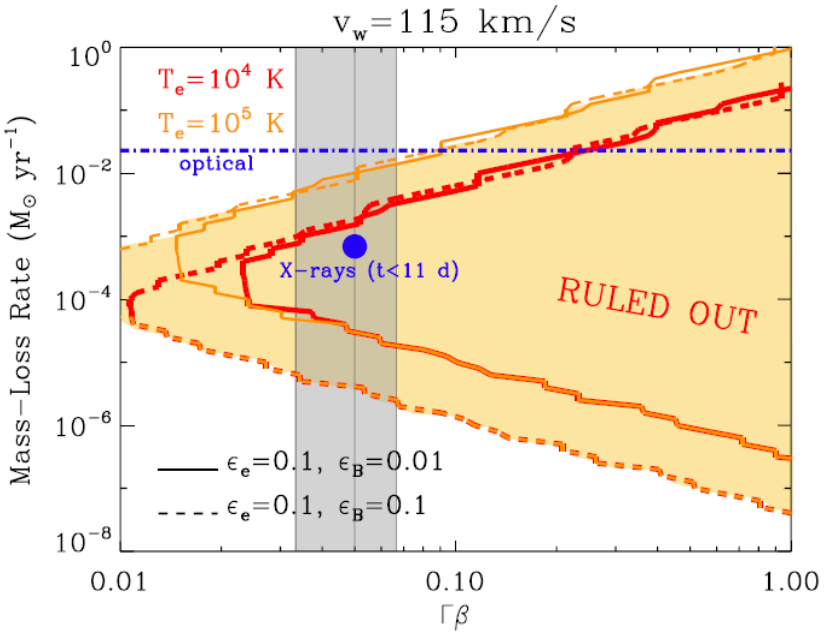
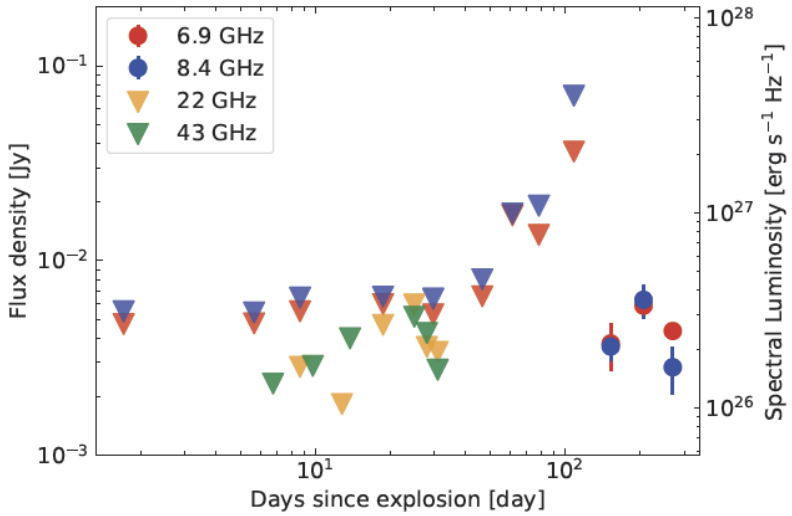
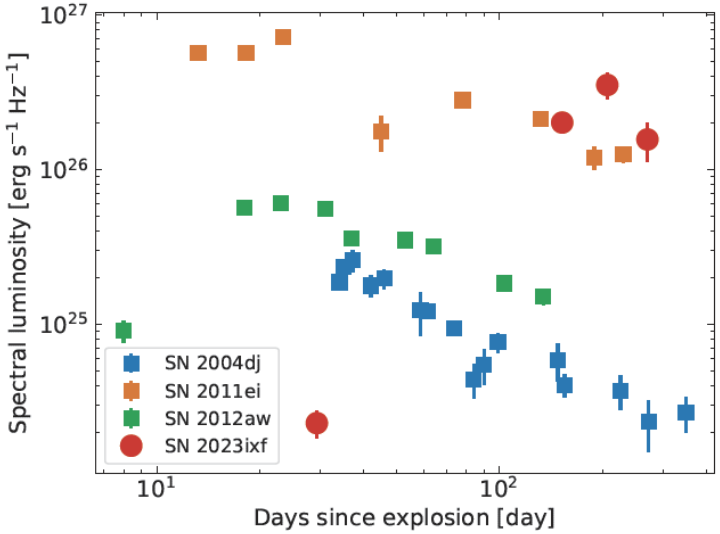


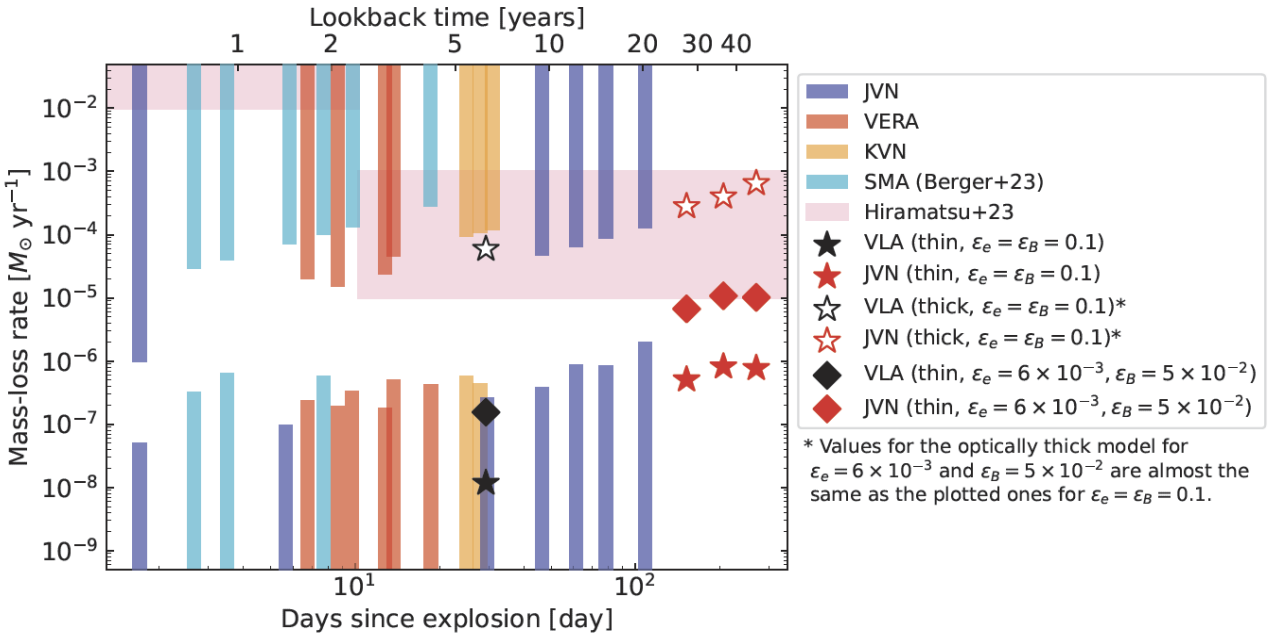
Figure 3. The phase space of progenitor mass-loss rate vs. ejecta velocity that is *excluded* by our most constraining SMA limits at 2.7, 7.7, and 18.6 days. The models (Chevalier 1998) assume $v_w = 115$ km s^{-1} (Smith et al. 2023) and are shown for two sets of equipartition parameters (ϵ_e and ϵ_B), an electron power-law distribution with $N_e(\gamma_e) \propto \gamma_e^{-p}$ with $p = 3$, a volume filling factor of 0.5, and two values for the electron temperature (T_e). The vertical gray shaded region indicates an ejecta velocity range of $v_{ej} = (1-2) \times 10^4$ km s^{-1}. The blue dot marks the value of $\dot{M}$ inferred from X-ray observations acquired at $\lesssim$11 days (Grefenstette et al. 2023), while the horizontal blue dotted–dashed line marks the value of $\dot{M}$ inferred from optical spectra at $\lesssim$14 days (Jacobson-Galan et al. 2023). Both values have been updated to $v_w = 115$ km s^{-1}.

Radio Follow-up Observations of SN 2023ixf by Japanese and Korean VLBIs

Yuhei Iwata [1,2] Masanori Akimoto,[3] Tomoki Matsuoka [4] Keiichi Maeda [5] Yoshinori Yonekura [6]
Nozomu Tominaga [1,7,8] Takashi J. Moriya [1,9] Kenta Fujisawa [10] Kotaro Niinuma [10,11]
Sung-Chul Yoon [12] Jae-Joon Lee [13] Taehyun Jung [13] and Do-Young Byun [13]







In this case, the mass-loss rate of the progenitor is estimated to have increased from ~ 10^{-6}–10^{-5} M_{sun} yr^{-1} to ~ 10^{-4} M_{sun} yr^{-1} between 28 and 6 years before the explosion.

Early-time millimeter observations of the nearby Type II SN 2024ggi @7Mpc

Maokai Hu [1], Yiping Ao [2,3] Yi Yang [1], Lei Hu [4], Fulin Li [2], Lifan Wang [5] and Xiaofeng Wang [1]

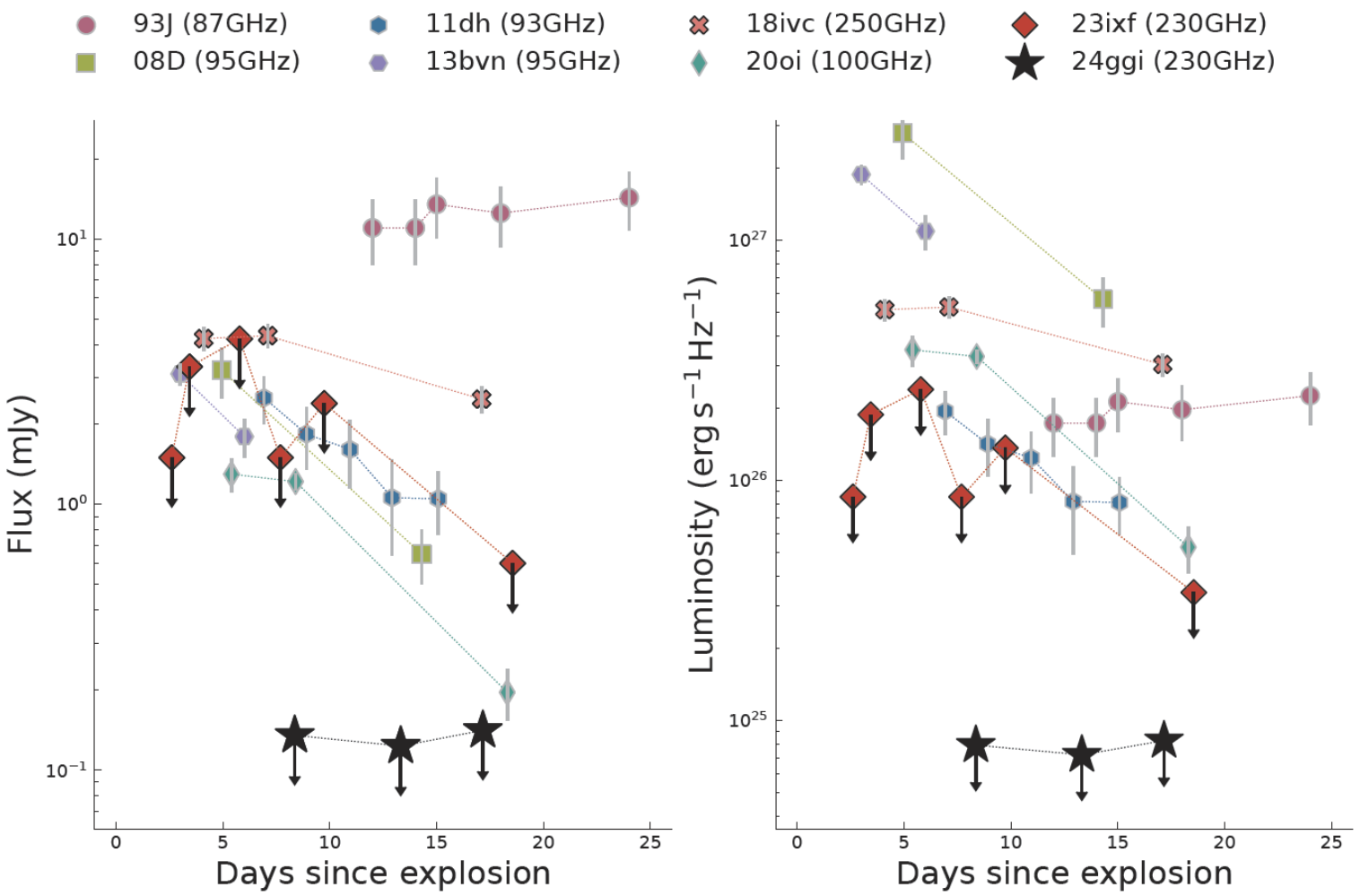
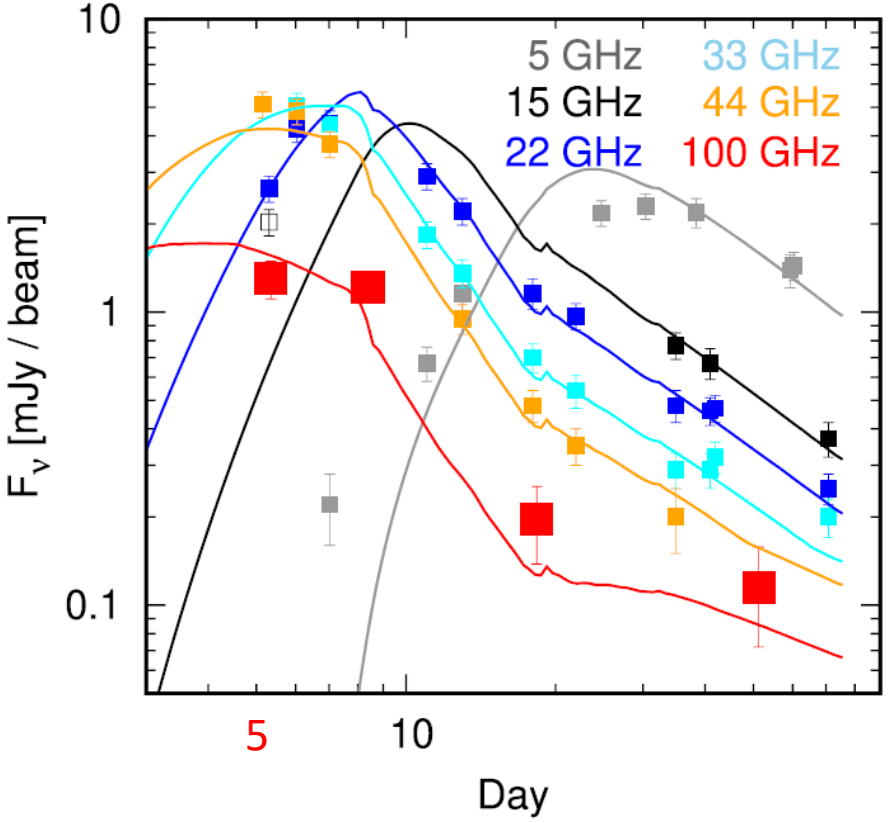


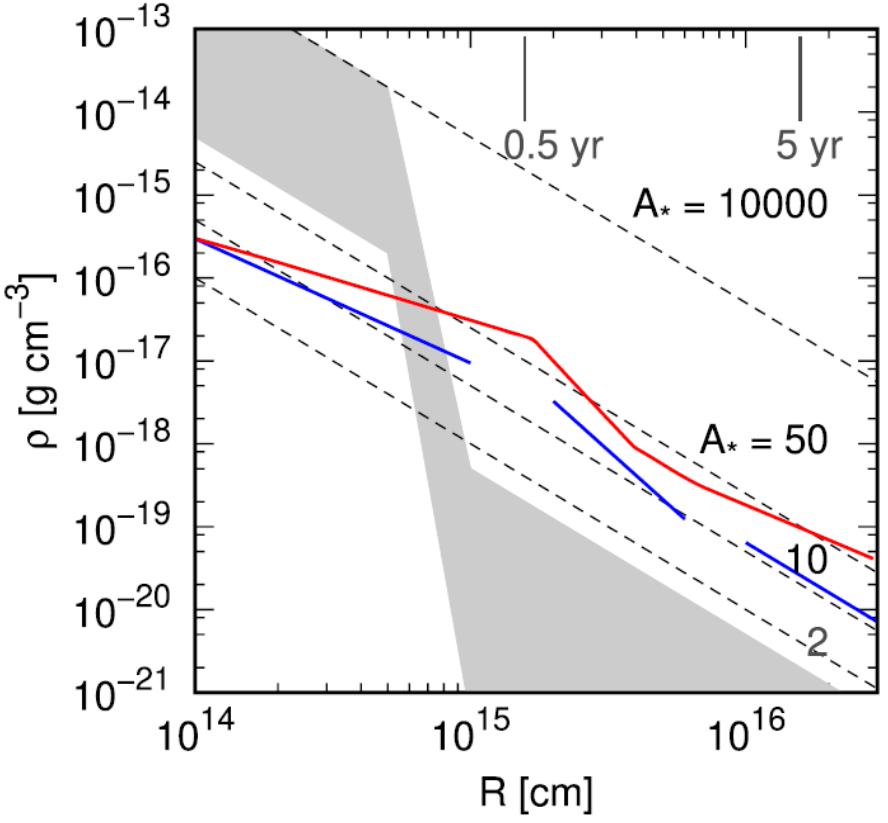
Figure 2. Left panel: the early-time millimeter-band observations of core-collapse SNe, including SN 1993J (Phillips et al. 1993; Weiler et al. 2007), SN 2008D (Soderberg et al. 2008; Gorosabel et al. 2010), SN 2011dh (Horesh et al. 2013), iPTF13bvn (Cao et al. 2013), SN 2018ivc (Maeda et al. 2023), SN 2020oi (Maeda et al. 2021), SN 2023ixf (upper limits, Berger et al. 2023), and SN 2024ggi (3σ upper limits). The corresponding luminosity is shown in the right panel.

The Final Months of Massive Star Evolution from the Circumstellar Environment around SN Ic 2020oi

@14-20Mpc

The inferred nonsmooth CSM distribution corresponds to fluctuations on the subyear timescale in the mass-loss history toward the SN explosion. Our finding suggests that the pre-SN activity is likely driven by the accelerated change in the nuclear burning stage in the last moments just before the massive star's demise.



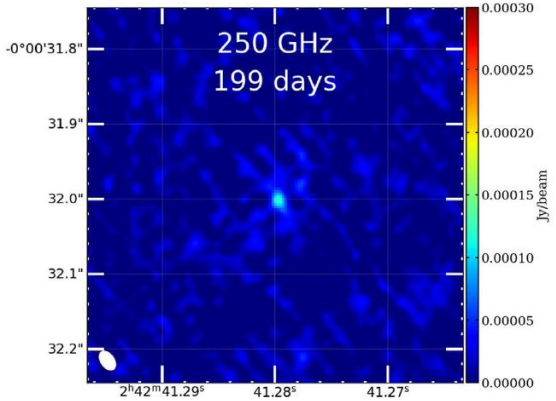


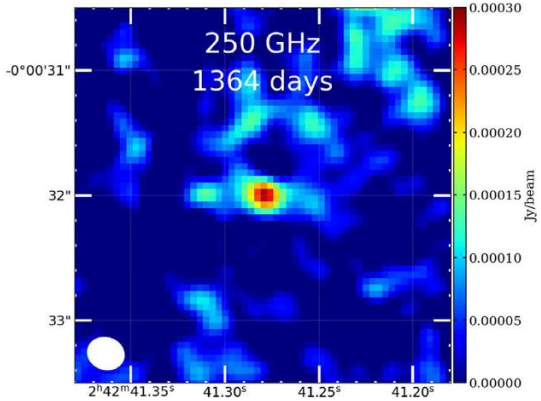
$$\rho_{\rm csm} = 5 \times 10^{11} A_* r^{-2}$$

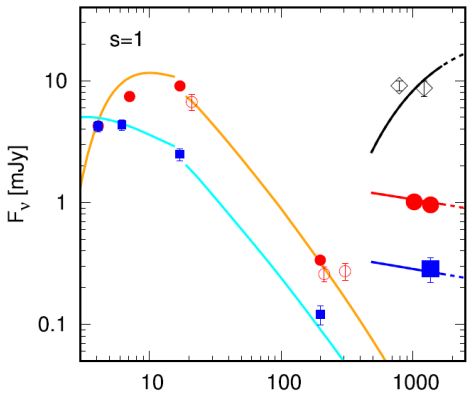
$$A_* = (\dot{M}/10^{-5}\,M_\odot\,{\rm yr}^{-1})/(v_{\rm w}/1{,}000\ {\rm km\ s}^{-1})$$

Maeda+21

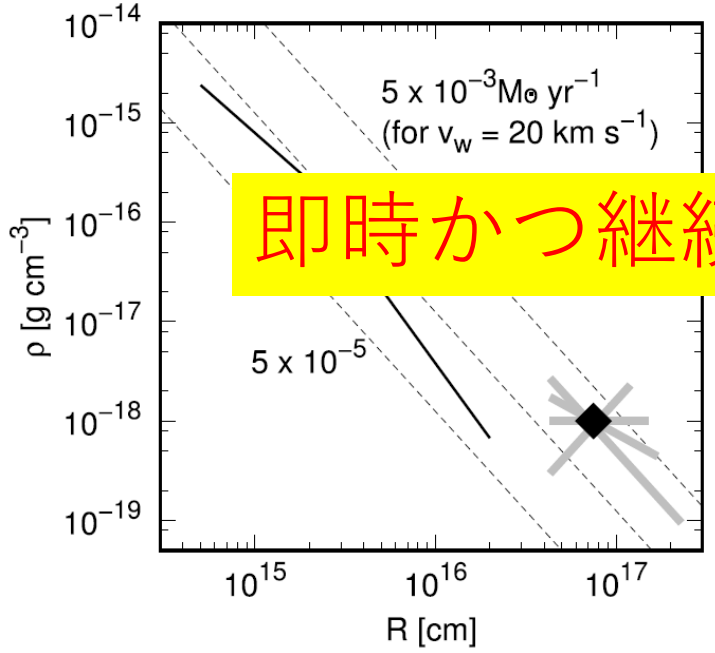
Resurrection of Type IIL Supernova 2018ivc: Implications for a Binary Evolution Sequence Connecting Hydrogen-rich and Hydrogen-poor Progenitors

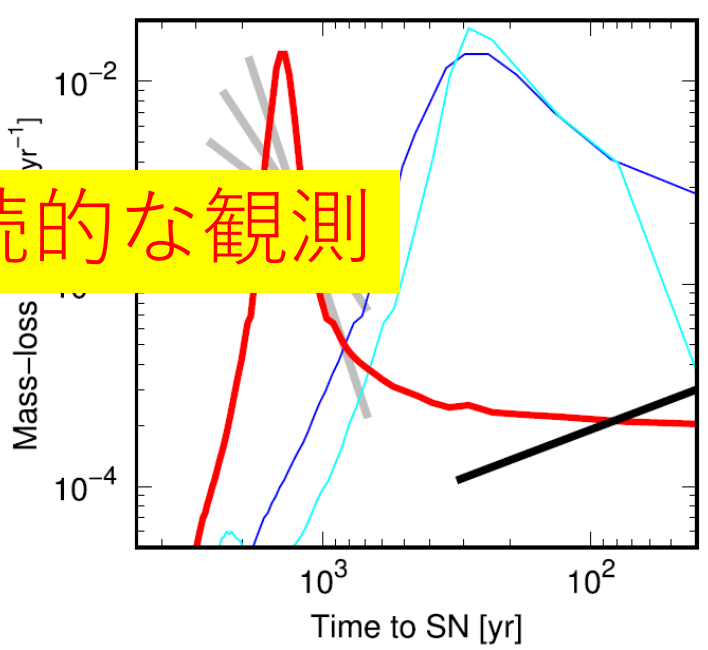






@10Mpc



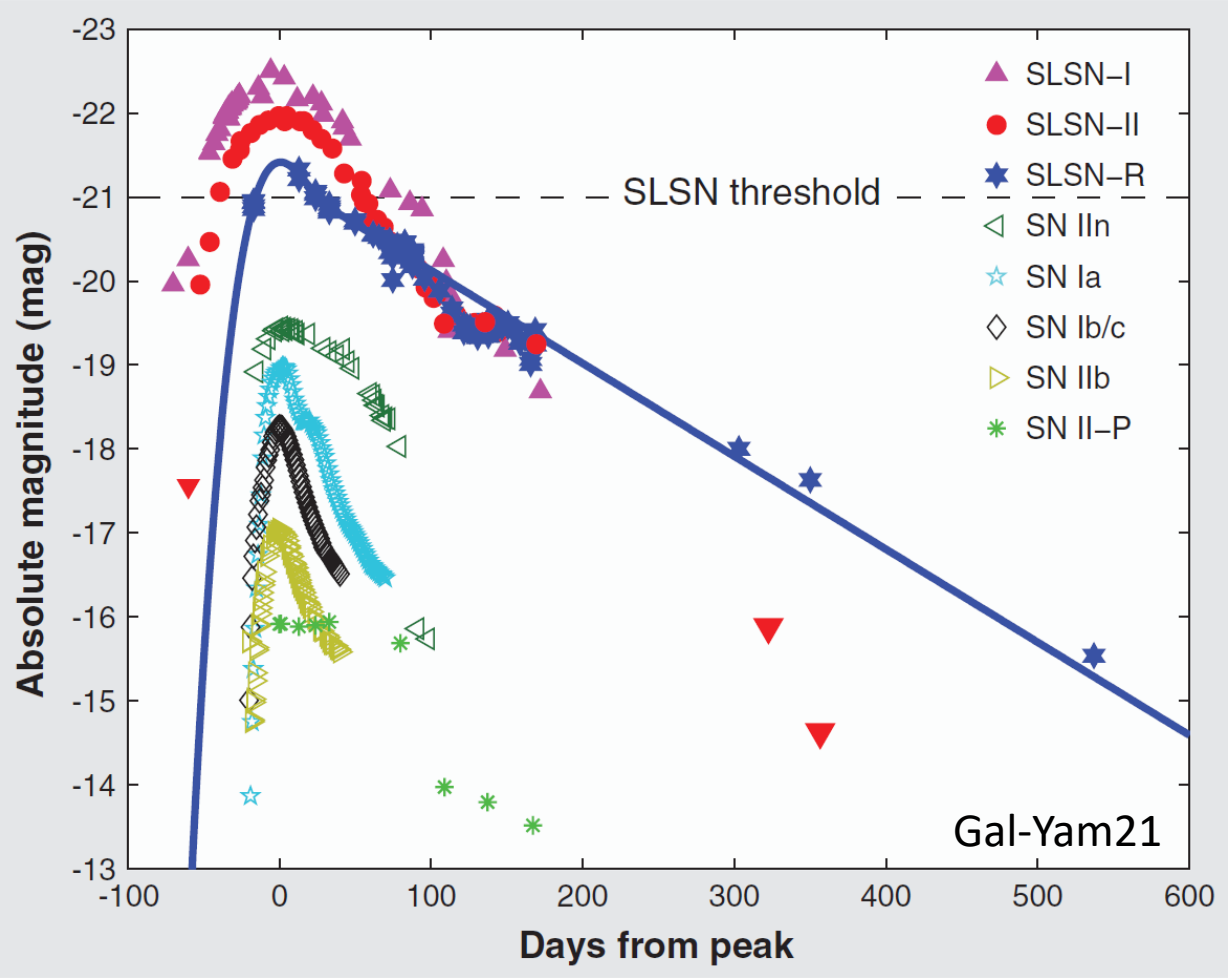


即時かつ継続的な観測

- The progenitor of SN 2018ivc had experienced a very high mass-loss rate (10^{-3} Msun yr^{-1}) ~1500 yr before the explosion, which was followed by a moderately high mass-loss rate (10^{-4} Msun yr^{-1}) up until the explosion.

Maeda+23

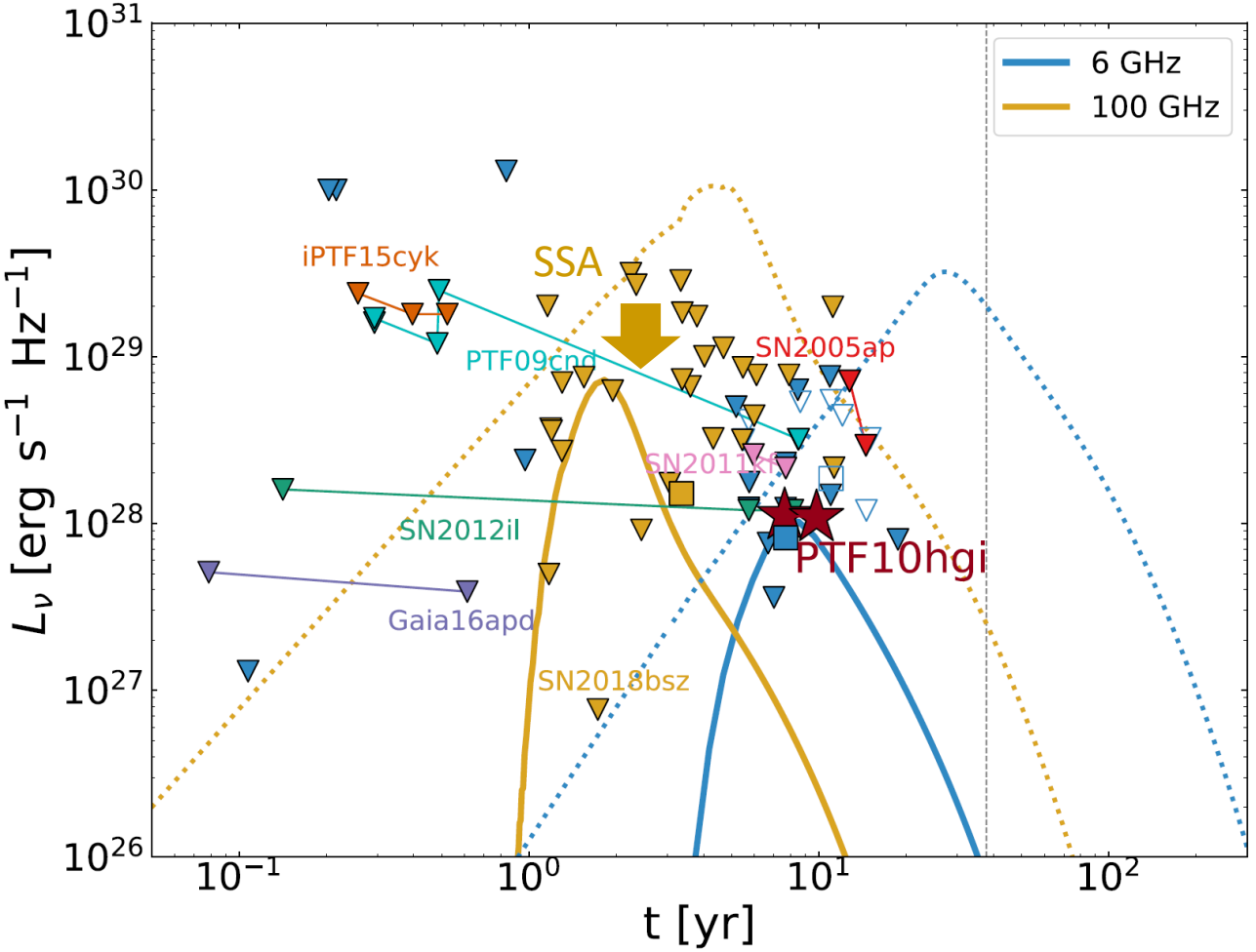
Superluminous supernovae



Energy source?

Magnetar, CSM interaction, or radioactivity

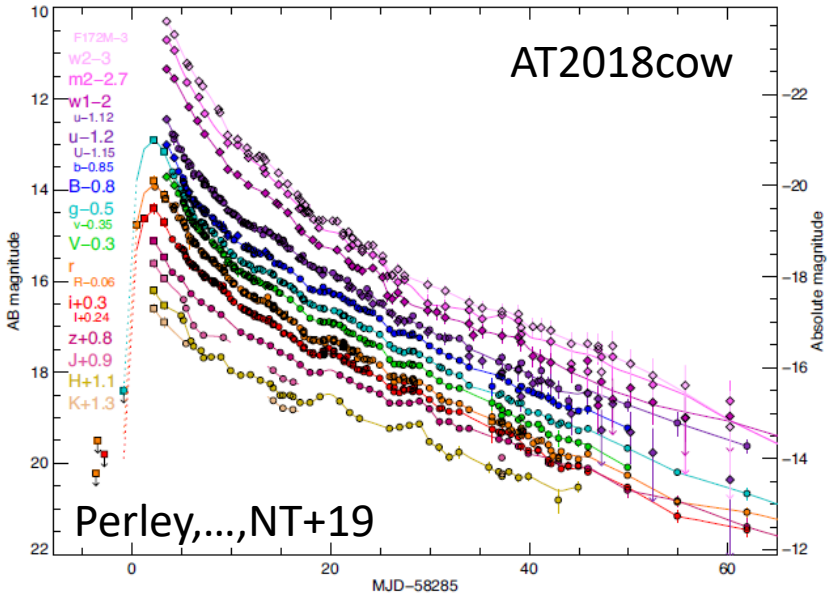
Late-time Radio and Millimeter Observations of Superluminous Supernovae and Long Gamma-Ray Bursts: Implications for Central Engines, Fast Radio Bursts, and Obscured Star Formation



- Among 43 sources at 6 and 100 GHz on a timescale of ~ 1–19 yr post-explosion. No radio/millimeter emission was detected except for 2 sources.
- A comparison to theoretical models suggests that continued radio monitoring may lead to detections of persistent radio emission on timescales of > a decade.

Eftekhari+21

Fast Blue Optical Transients

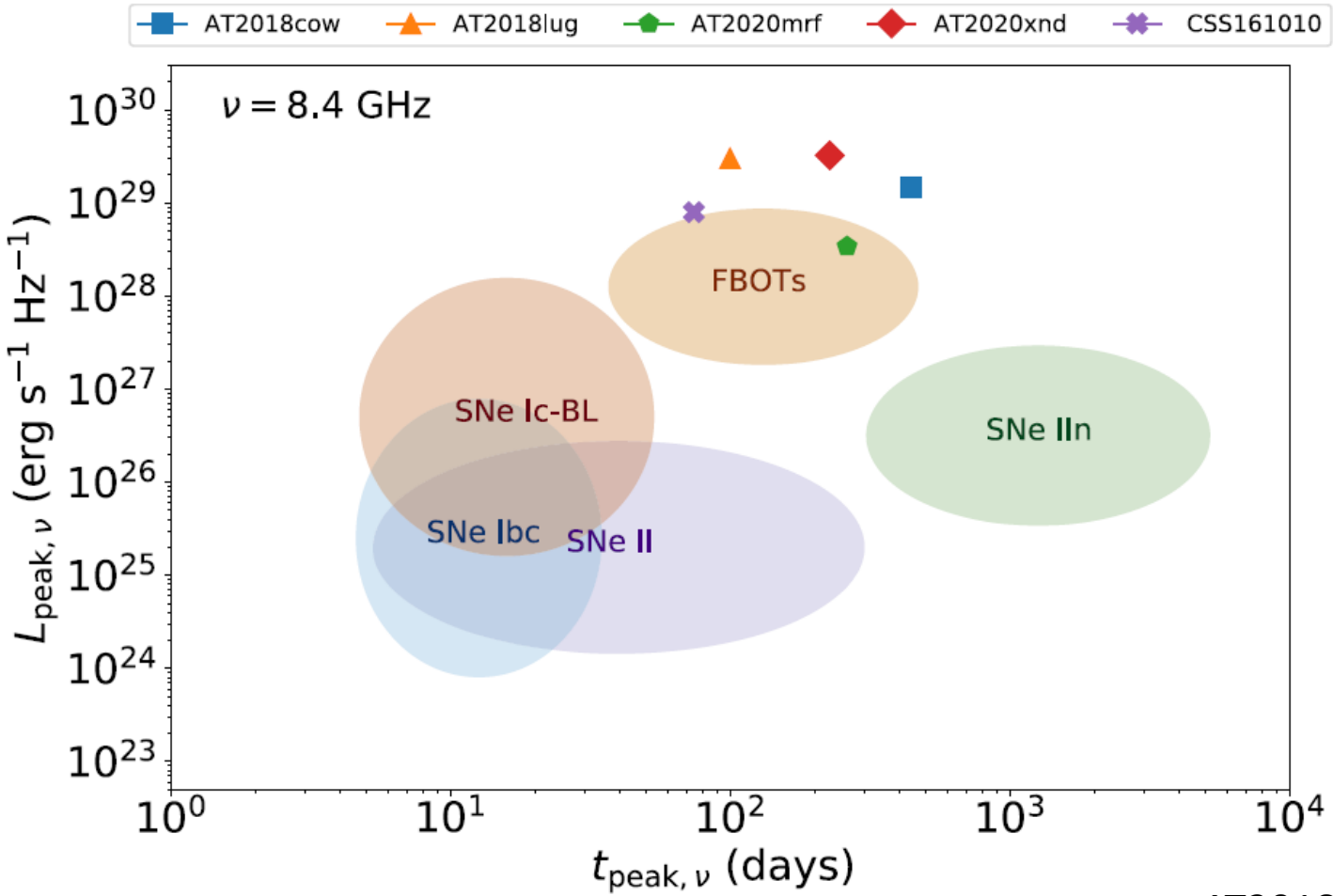


Ultra-striped SNe?
Accretion disk around BHs?

The Astrophysical Journal, 946:35 (7pp), 2023 March 20 https://doi.org/10.3847/1538-4357/acbb04
© 2023. The Author(s). Published by the American Astronomical Society.
OPEN ACCESS

A Population Study of the Radio Emission of Fast Blue Optical Transients

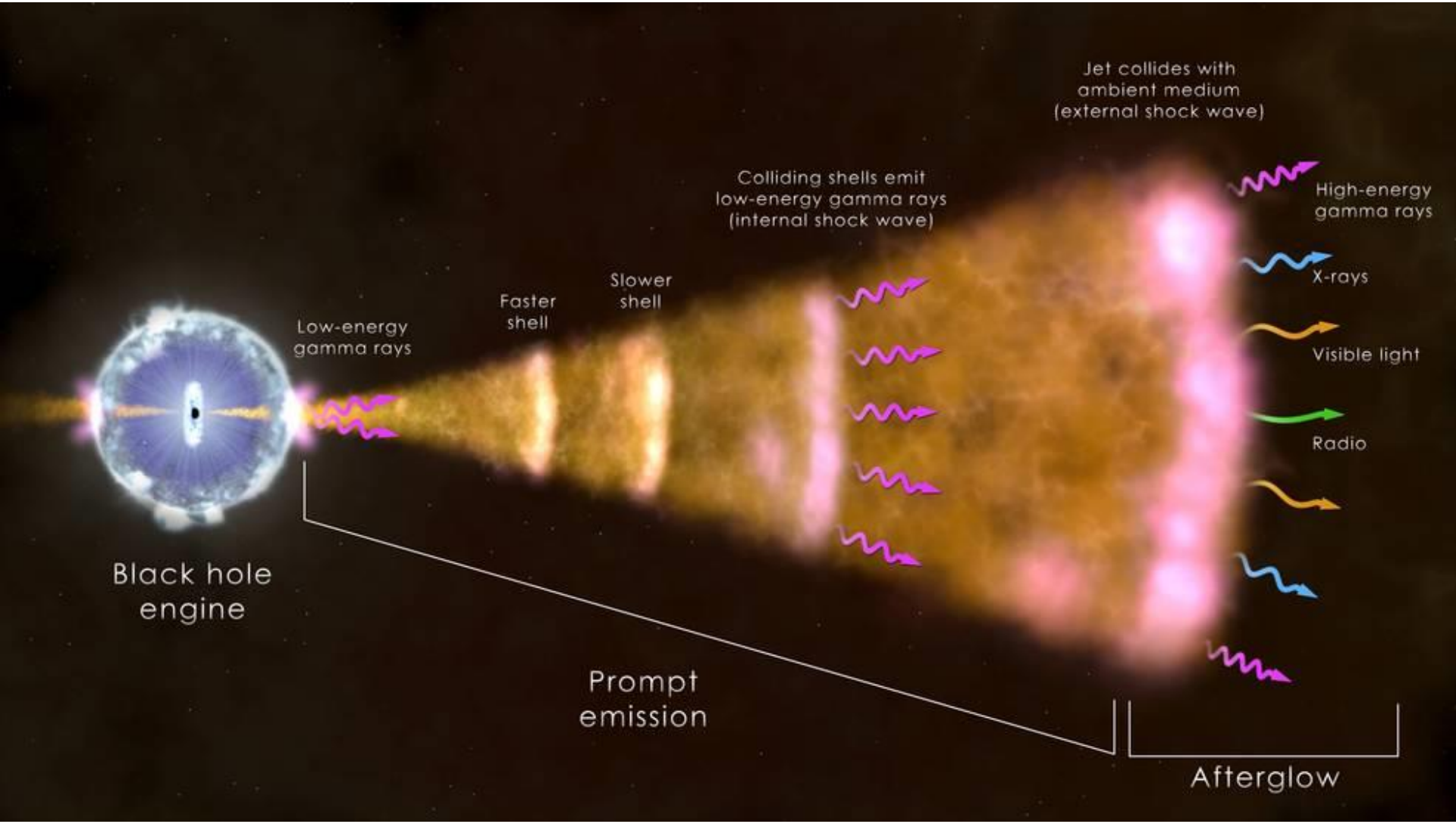
Jian-Feng Liu (刘建峰)[1,2], Liang-Duan Liu (刘良端)[1,2], Yun-Wei Yu (俞云伟)[1,2], and Jin-Ping Zhu (朱锦平)[3]
[1] Institute of Astrophysics, Central China Normal University, Wuhan 430079, People's Republic of China; liuld@ccnu.edu.cn, yuyw@ccnu.edu.cn
[2] Key Laboratory of Quark and Lepton Physics, Central China Normal University, Ministry of Education, Wuhan 430079, People's Republic of China
[3] School of Physics and Astronomy, Monash University, Clayton, VIC 3800, Australia
Received 2022 September 30; revised 2023 January 10; accepted 2023 February 8; published 2023 March 24



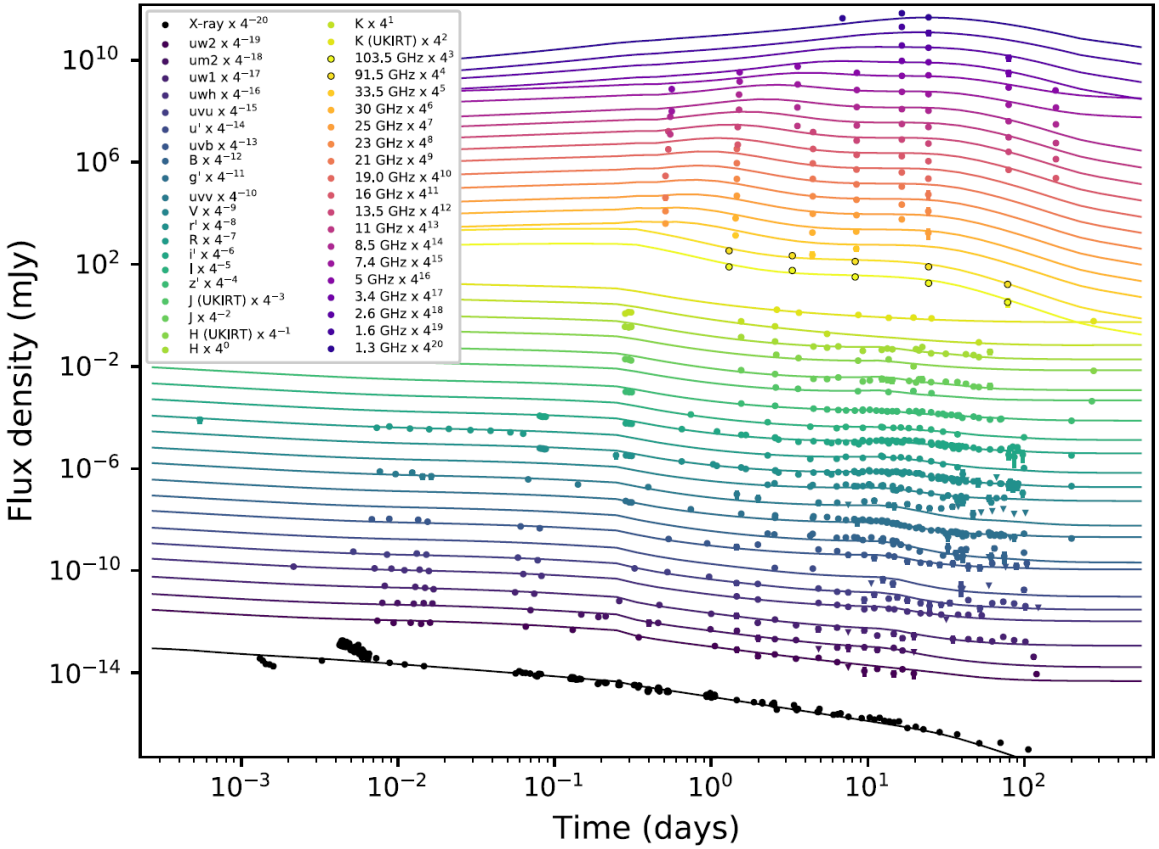
AT2018cow@60Mpc

Gamma-ray bursts

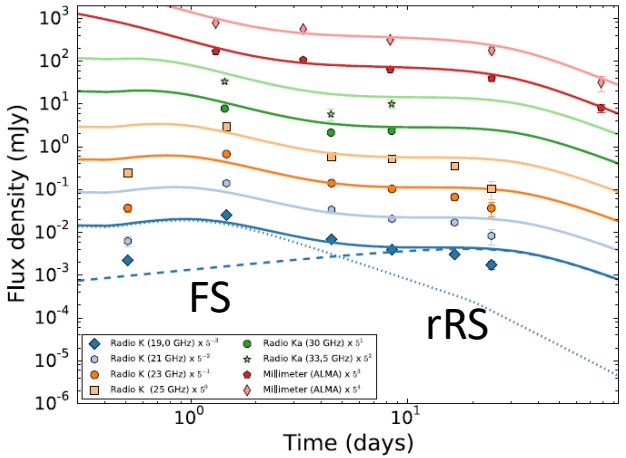
Schematic view of GRBs



First ALMA Light Curve Constrains Refreshed Reverse Shocks and Jet Magnetization in GRB 161219B



@z=0.1475 (700Mpc)



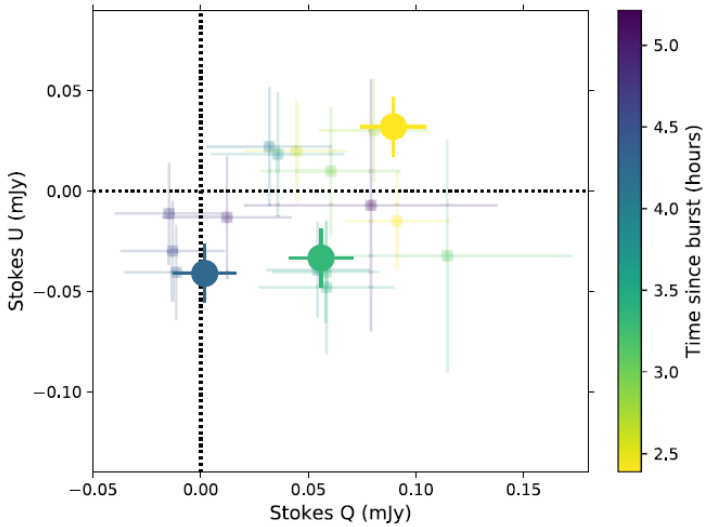
- The centimeter- and millimeter-band observations before 8.5 days require emission in excess of that produced by the afterglow forward shock (FS). These data are consistent with radiation from a refreshed reverse shock (RS) produced by the injection of energy into the FS, signatures of which are also present in the X-ray and optical light curves.
- These direct, multifrequency measurements of a refreshed RS spanning the optical to radio bands highlight the impact of radio and millimeter data in probing the production and nature of GRB jets.

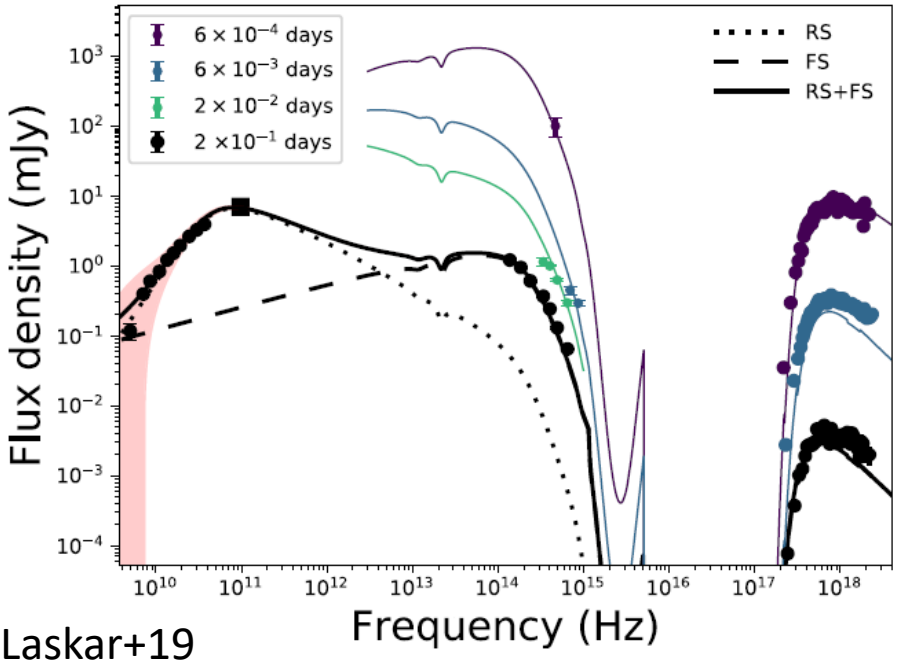
Laskar+18

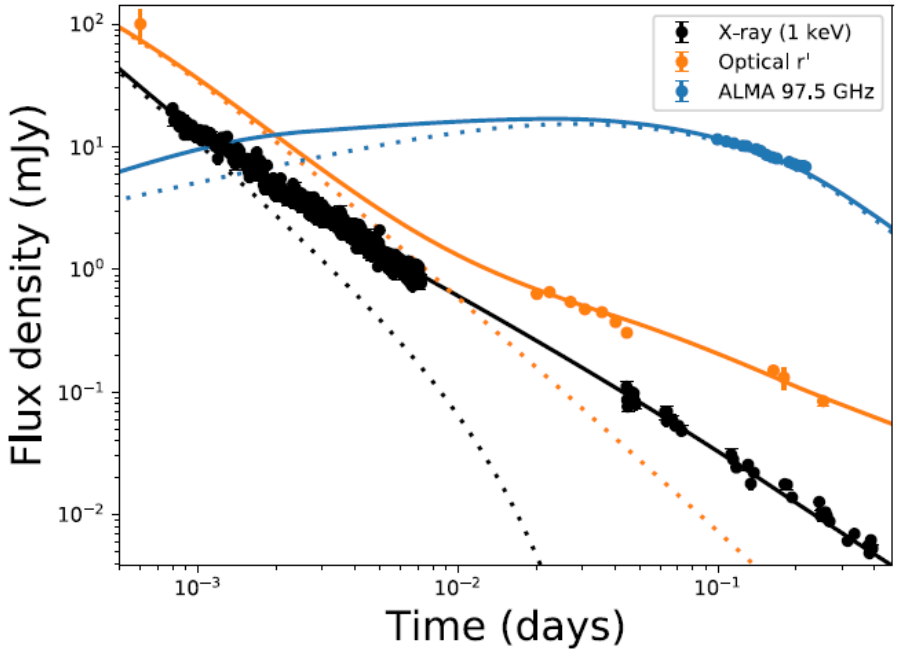
ALMA Detection of a Linearly Polarized Reverse Shock in GRB 190114C

@z=0.4245 (2.3Gpc)

- Linear polarization is detected at the ≈5σ level, decreasing from Π=0.87+-0.13% to 0.60+-0.19%, and evolving in polarization position angle from 10+-5deg to -44+-12deg during the course of the observations.
- The coherence scale of tangled magnetic fields in the ejecta to an angular size of ~10^{-3} radian, while the rotation of the polarization angle rules out the presence of large-scale, ordered axisymmetric magnetic fields, and in particular a large-scale toroidal field, in the jet.



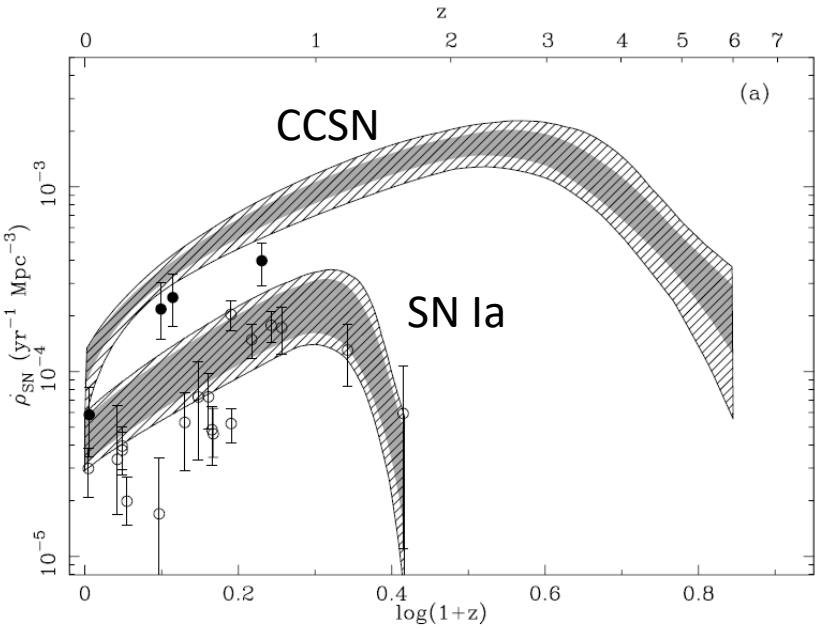




Laskar+19

Number estimate

- CCSN rate: 10^{-4} SN/yr/Mpc^3
  - 0.5 SN @<10Mpc
- 1mJy
  - @ 10Mpc -> 1e26 erg/s/Hz
  - @ 100Mpc -> 1e28 erg/s/Hz



Hopkins&Beacom06

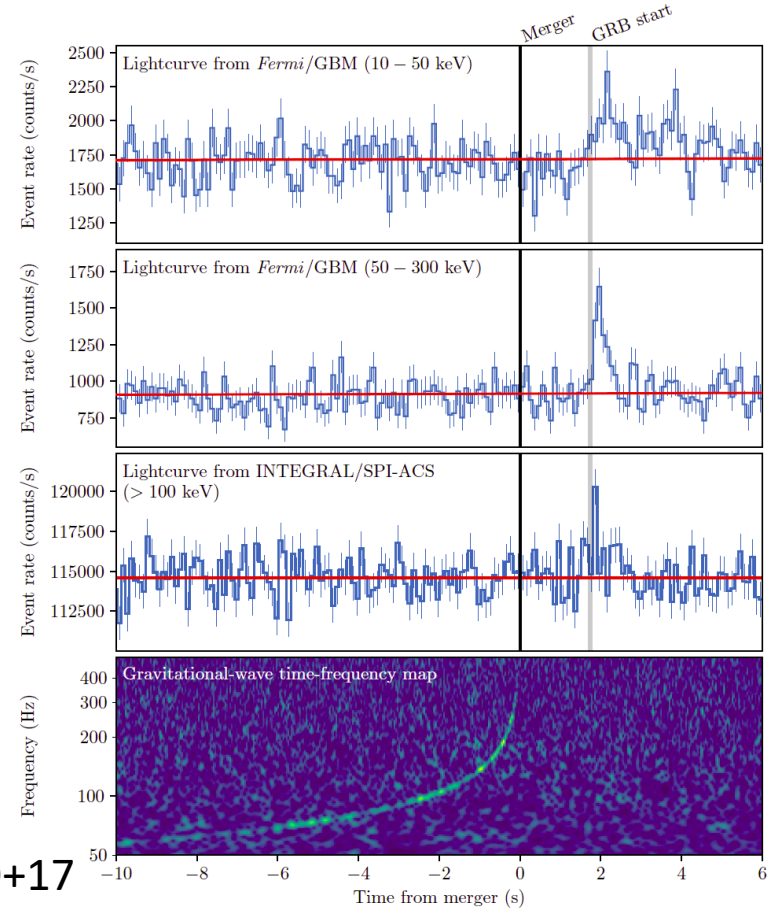
- SLSN: 0.1 % of SN (Prajs+16)
- FBOT: 0.1% of SN (Ho+23)
- GRB: 0.01% of SN (Finke+24)
  - Low-luminosity GRB: 0.1% of SN (Virgili+09)

Multi-messengers

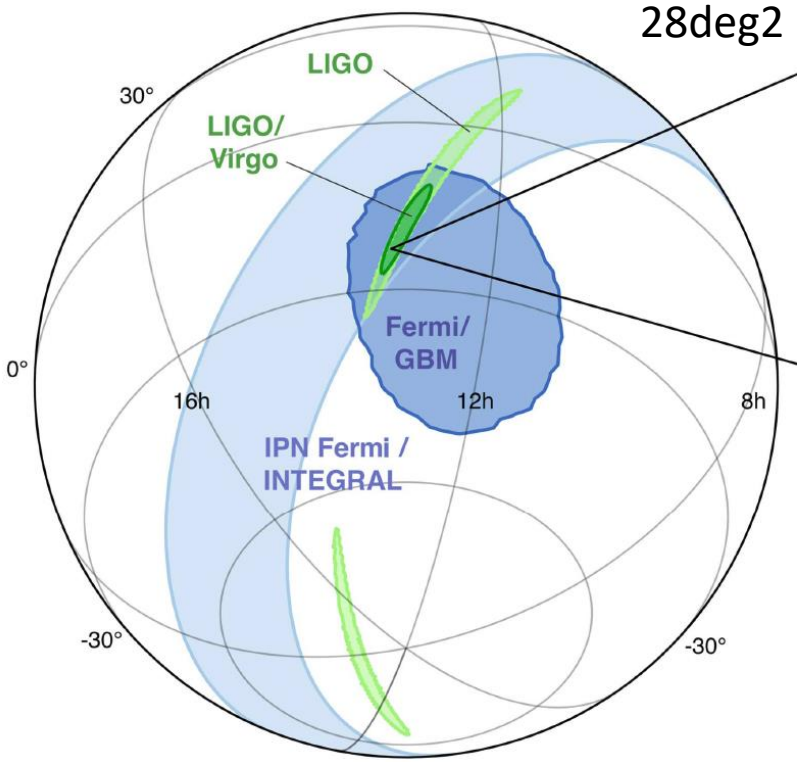
Gravitational wave

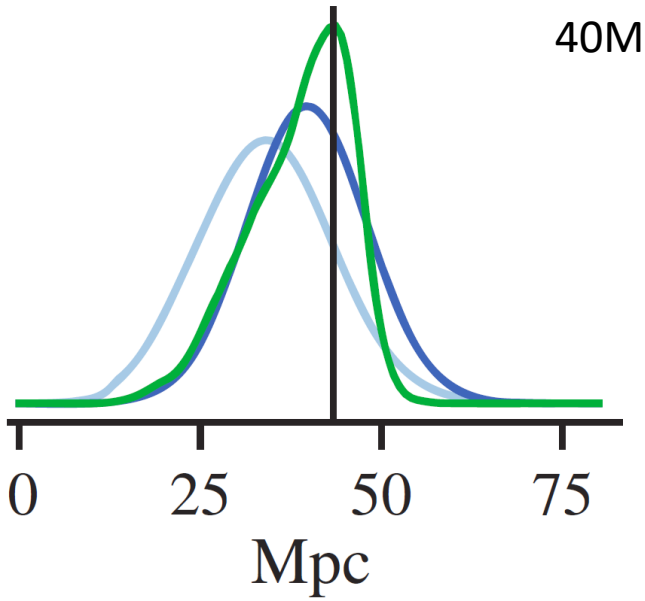
GW170817 - NSM

NS masses are 1.17–1.60 $M_\odot$, with the total mass of the system $2.74^{+0.04}_{-0.01} M_\odot$.



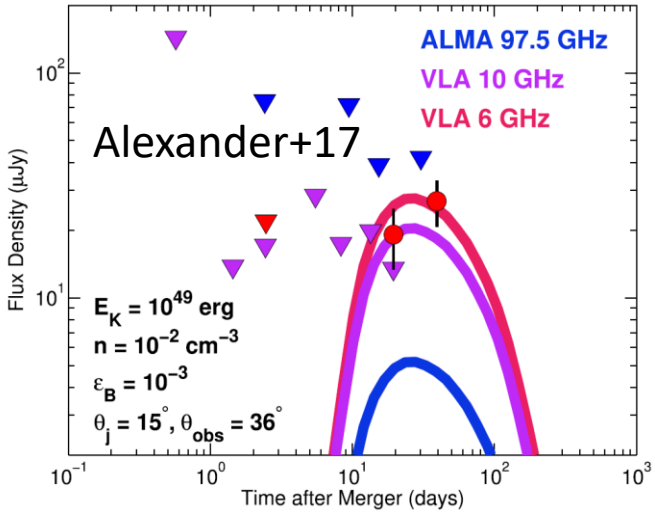
LIGO+17

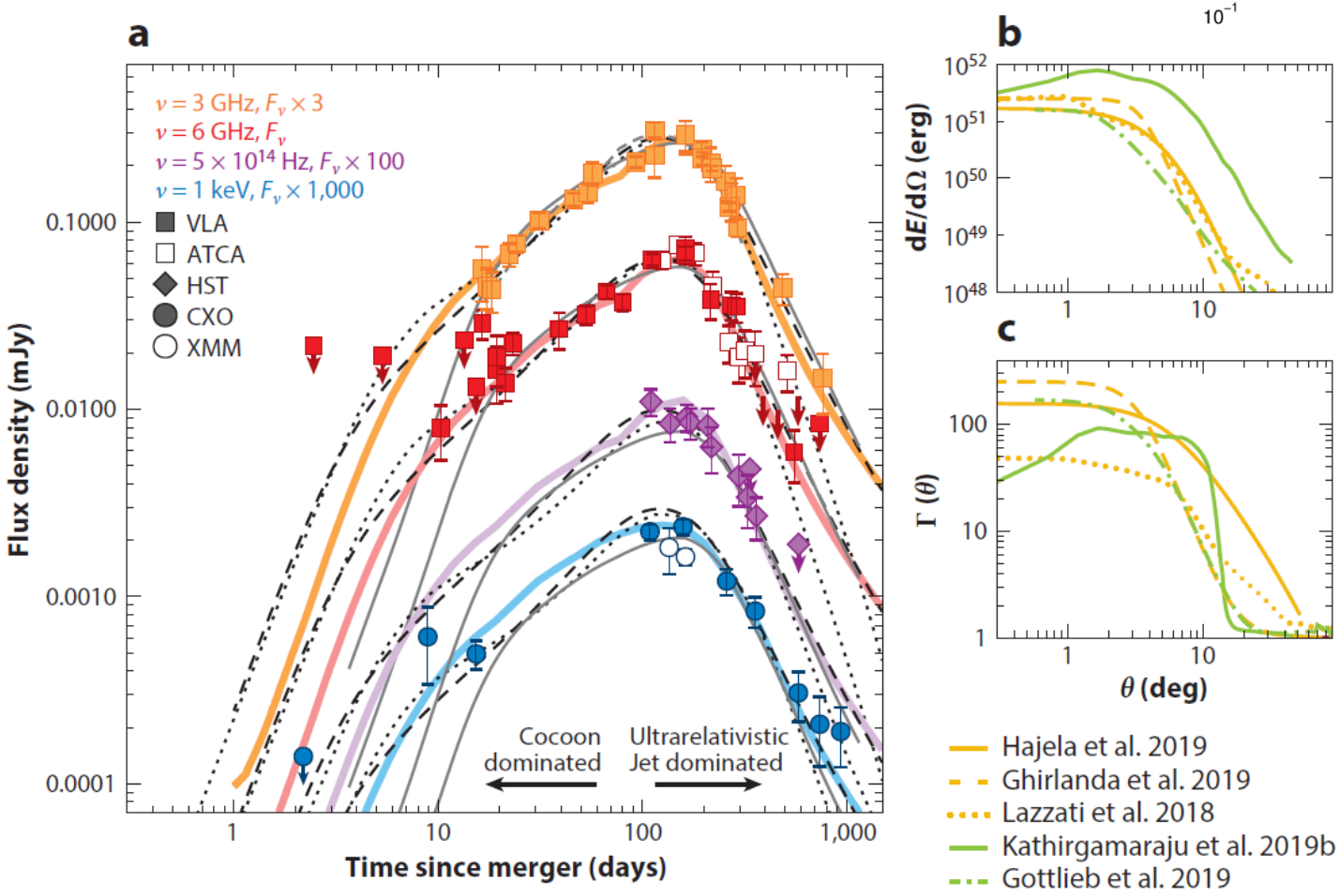




Radio observations in multi-messenger astronomy

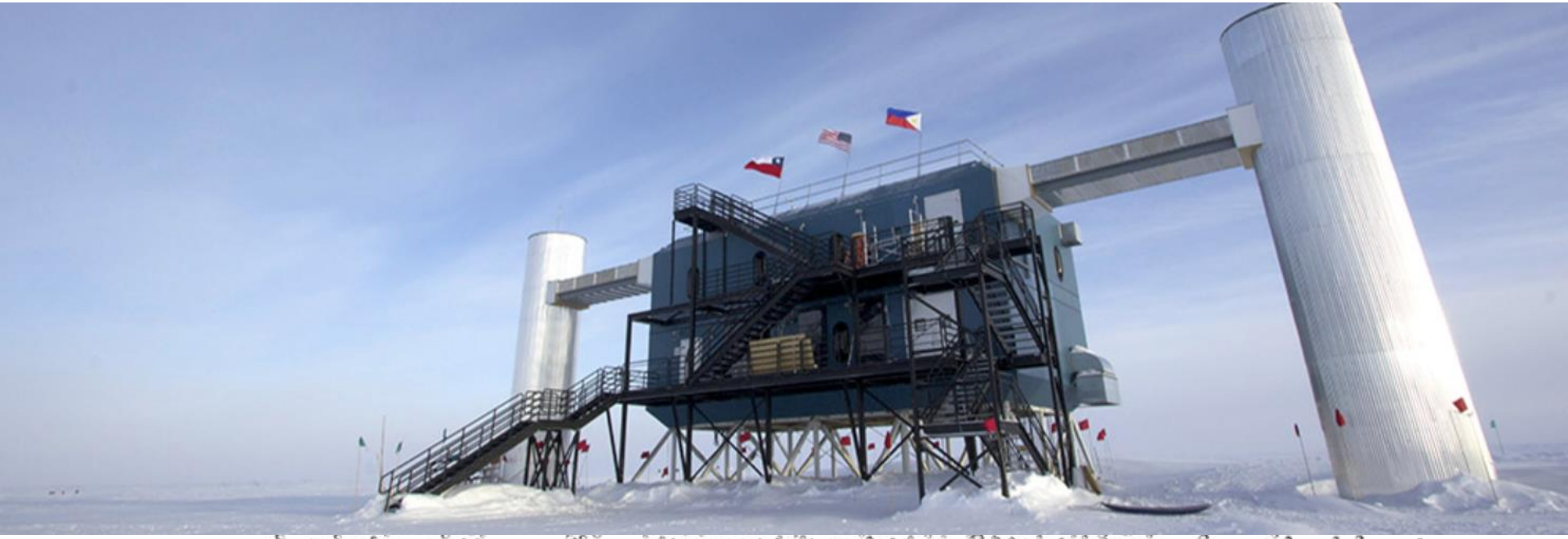
@40Mpc

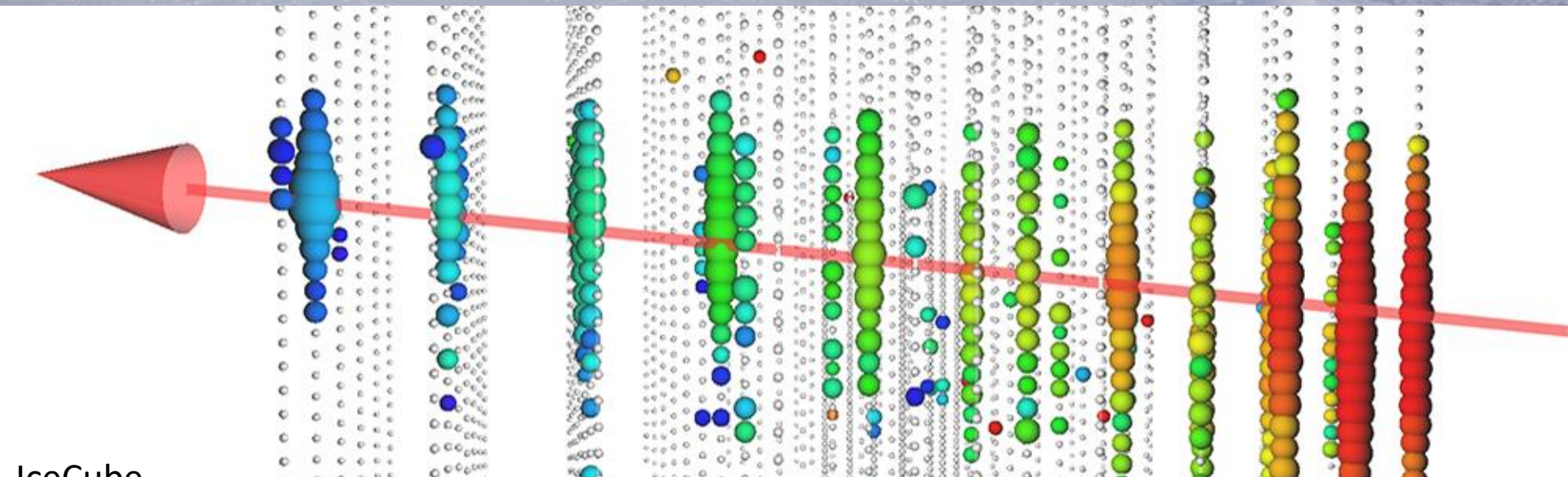




Margutti & Chornock 21

High-energy neutrinos

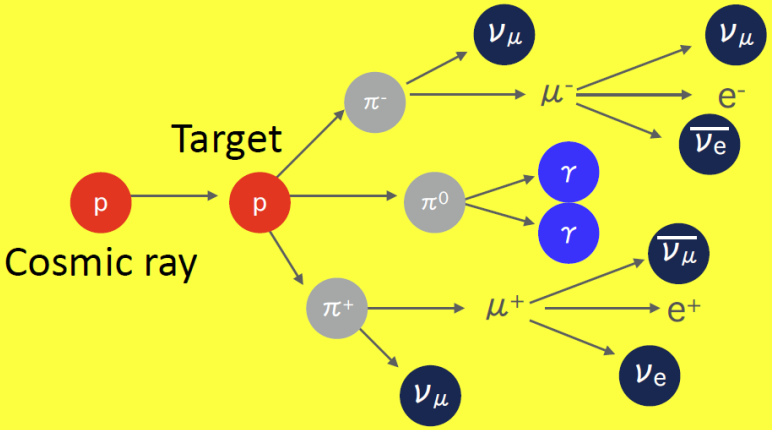




IceCube

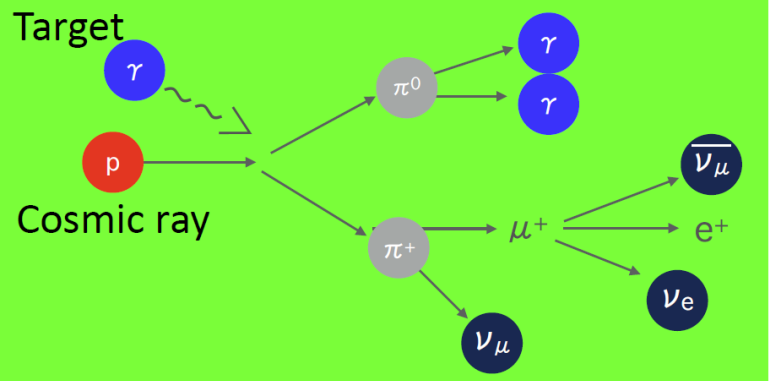
High-E neutrino production

- pp inelastic collision



- p+p → p+p+π
- $\pi^{\pm}$→ 3ν+e
- π^0→2γ

- Photomeson production (pγ)



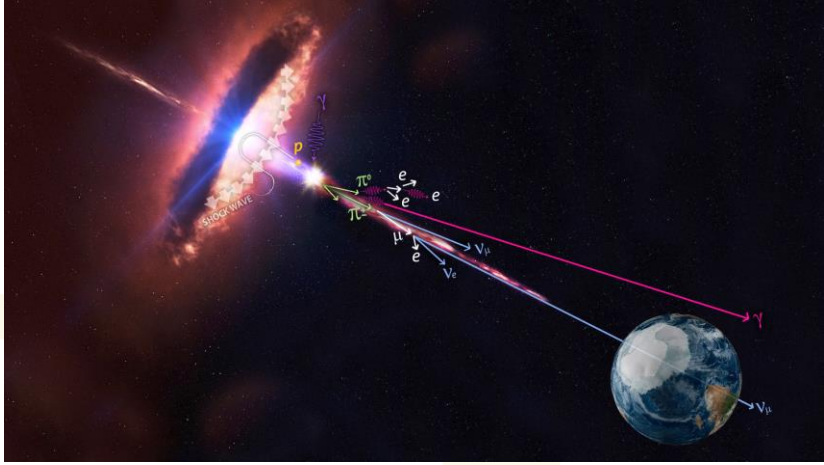
- p+γ → p+π
- $\pi^{\pm}$→ 3ν+e
- π^0→2γ

Interaction between CRs & photons/nuclei → Neutrino production

Gamma-rays inevitably accompanied with neutrinos

Kimura+

Origin of cosmic rays



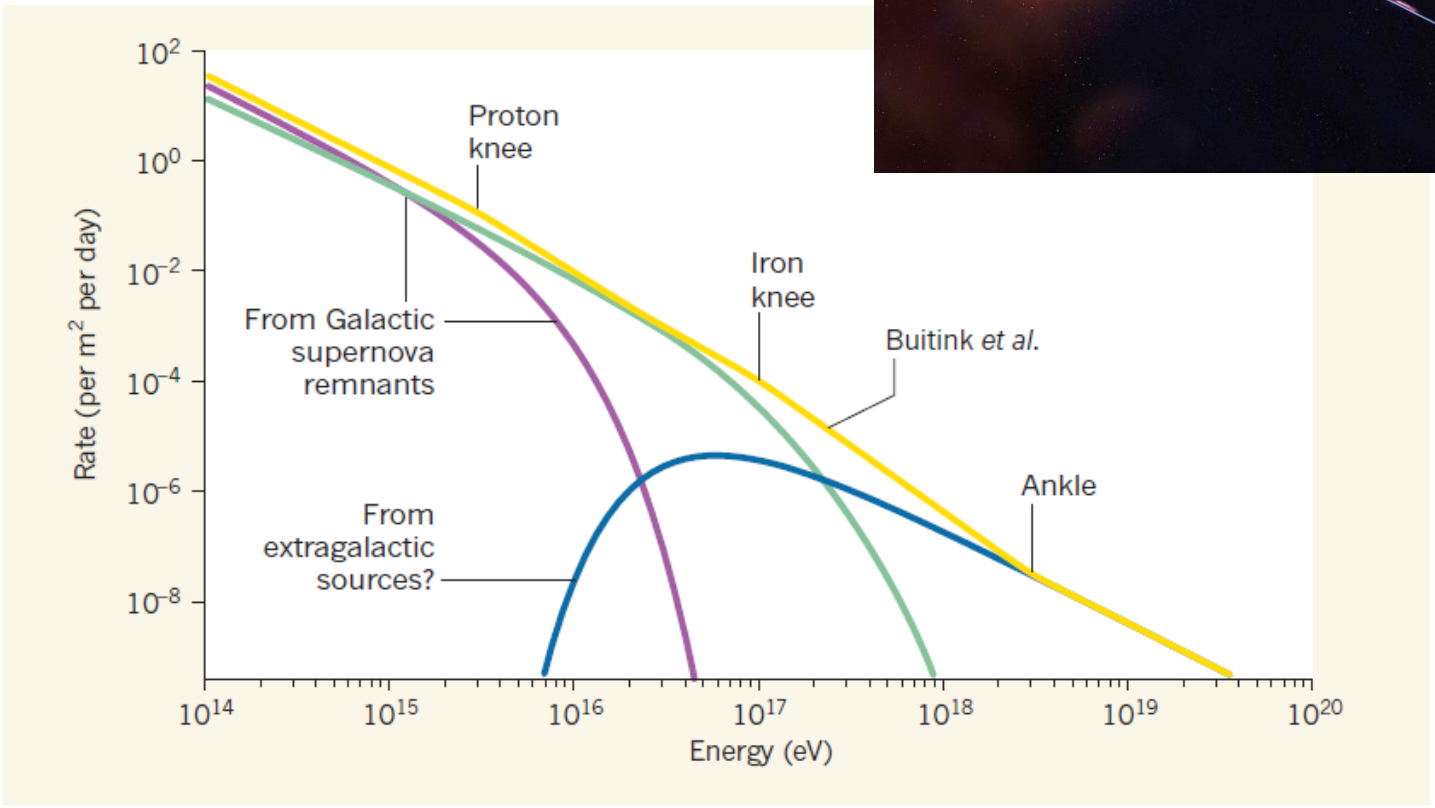
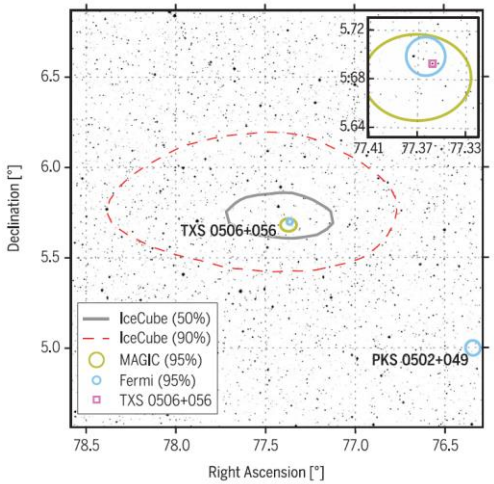


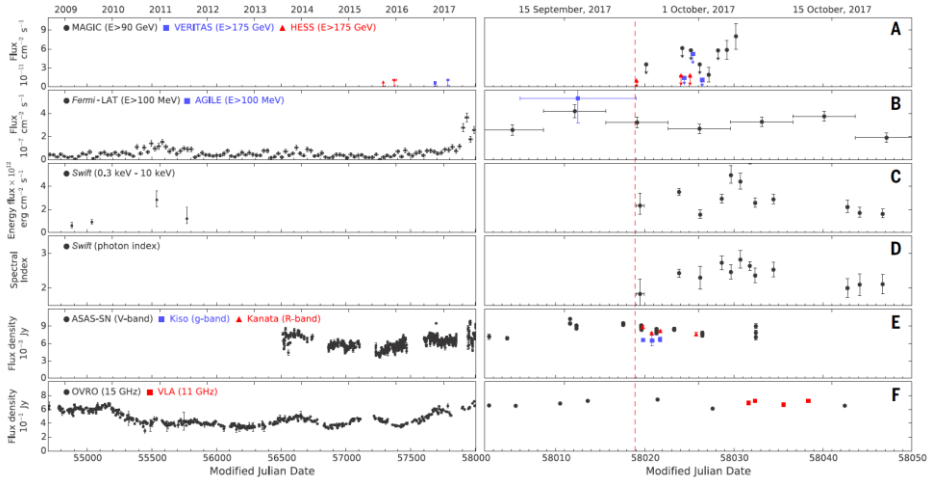
Figure 1 | The energy spectrum of cosmic rays. When the number of cosmic rays per square metre that arrive at Earth's surface per day is plotted on a logarithmic scale against the energies of the cosmic rays, also on a logarithmic scale, the overall graph (yellow line) between 10^{14} and 10^{19} electronvolts contains four distinct linear regions, connected by changes in slope called the proton knee, the iron knee and the ankle. The slope changes correspond to transitions between the composition or sources of cosmic rays that dominate at different energies. Buitink *et al.*[1] report on observations of cosmic rays between the iron knee and the ankle, providing clues about their origins.

Taylor+16

Origin of high-energy neutrinos

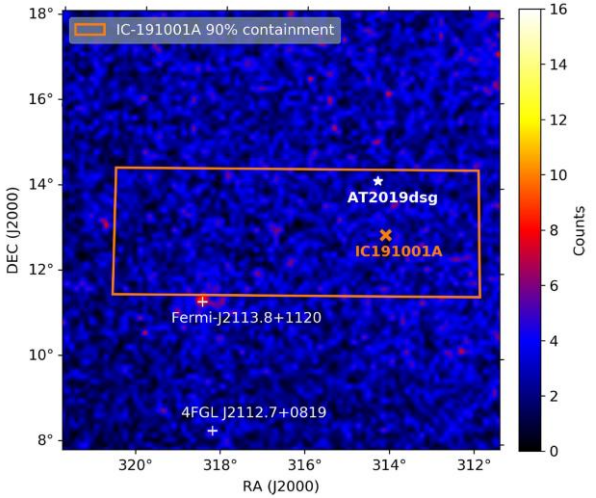
- Blazar TXS 0506+056

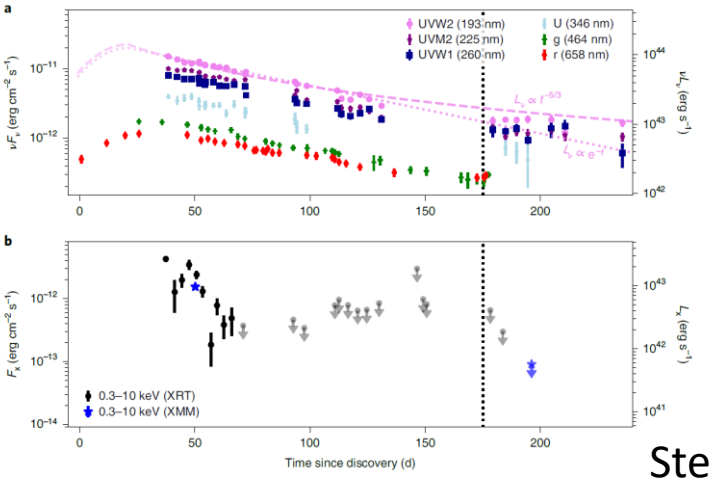




IceCube+18

- Tidal disruption event AT 2019dsg





Stein+21

Origin of high-energy neutrinos?

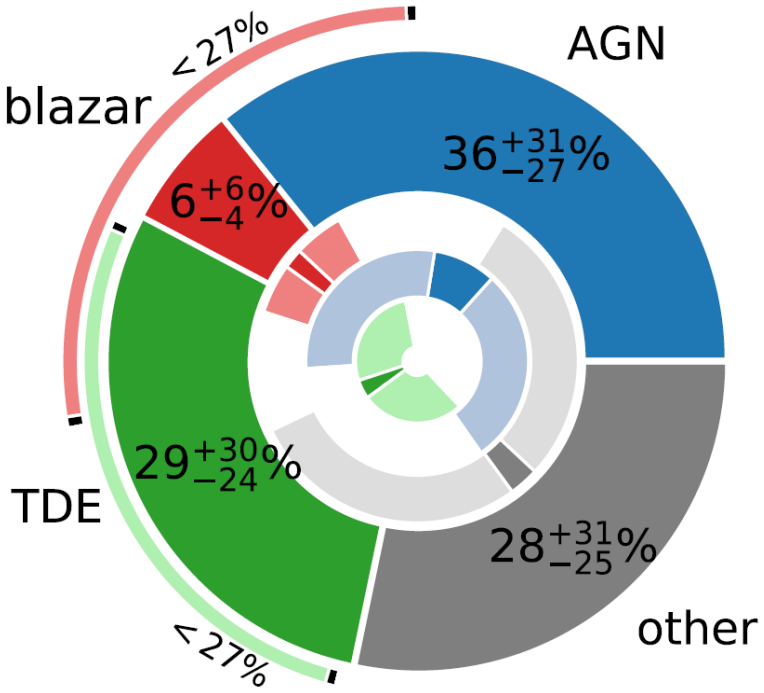


Figure 3. Pie chart of expected fraction of IceCube's neutrino flux from the three source types with directly associated neutrino detections, and the remaining flux from unknown sources (other). The main pie chart indicates the average expected fractional values, while the innermost charts indicate uncertainty by showing the minimum (dark) and maximum (light) extent of the fractional contributions allowed within the 90% credible regions. Outer thin slices further show independent observational constraints from stacking analyses for TDEs (Stein 2019) and blazars (Aartsen et al. 2017) that limit their contributions to <27% each at 90% confidence level.

Identification of EM counterparts

Bartos+21

Localization & number

- Gravitational waves (>10deg2, <200Mpc)
  - BNSM rate: 0.01-1% of SN
  - NSBH rate: 0.01-0.1% of SN (LIGO arXiv:2111.03634)
- High-energy neutrinos (~deg2, z>1)
  - But, multiplets (z<0.2, Yoshida+22)

	Gold events	Bronze Events
Signal ($E^{-2.19}$)	6.6 (Total) 5.1 (GFU) 0.5 (HESE) 2.1 (EHE)	8.4 (Total) 7.6 (GFU) 0.8 (HESE)
Atmospheric Backgrounds	6.1 (Total) 4.7 (GFU) 0.4 (HESE) 1.9 (EHE)	19.8 (Total) 18.5 (GFU) 1.3 (HESE)
Observed historical rate	9.9 (Total) 7.8 (GFU) 1.1 (HESE) 4.3 (EHE)	28.2 (Total) 26.2 (GFU) 2.0 (HESE)

[/yr/sky]

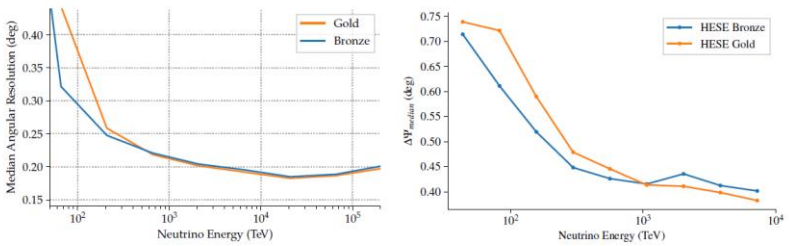


Figure 2: IceCube realtime astrophysical neutrino alert angular resolution as a function of neutrino energy. The left panel presents the angular resolution for through-going neutrino selections (GFU and EHE) and the right panel presents the angular resolution for the HESE starting track selection. Alerts at the Gold and Bronze levels are issued based on these selections, with a minimum reported angular resolution for automated alerts of 0.2 degress reported. In these figures, the Bronze alerts shown also include events selected by the Gold alerts.

GFU: Gamma-ray Follow-Up (GFU) track selection
HESE: High Energy Starting (HESE) selection
EHE: Extremely High Energy (EHE) alert selection

https://gcn.gsfc.nasa.gov/doc/IceCube_High_Energy_Neutrino_Track_Alerts_v2.pdf

まとめ

- Transient は主にシンクロトロン放射で光る
  - 高い周波数の観測はより困難
  - より初期（爆発直前）の情報が得られる
- 即時かつ継続的な観測
- 空振りにめげない心
  - Non-detection で何をするか

- SN: 0.5SN/yr @<10Mpc
  - SLSN, FBOT, (LL)GRB 0.5/yr @<100Mpc
- MMA
  - Poor localization, high-redshift
  - High-E neutrino multiplets